Comparative anatomy of the gill skeleton of fossil Aulopiformes (Teleostei: Eurypterygii)

Hermione Beckett[a*], Sam Giles[a], and Matt Friedman[a,b]

[a]Department of Earth Sciences, University of Oxford, South Parks Road, Oxford OX1 3AN, UK

[b]Current address: Museum of Paleontology and Department of Earth and Environmental Science, University of Michigan, 1109 Geddes Ave, Ann Arbor, MI 48109-1079, USA

*Correspondence to: Hermione Beckett, +44 (0) 1865 272000 hermione.beckett@earth.ox.ac.uk, Department of Earth Sciences, University of Oxford, Oxford, UK, OX1 3AN

Abstract

Gill skeletons provide a rich source of character information for inferring the relationships among extant fishes. However, the difficulties in accessing branchial structures in fossils have limited the use of gill-arch anatomy in phylogenetic studies of extinct fishes. Here we apply micro computed tomography (μCT) to visualize and describe gill-arch anatomy in three-dimensionally preserved Late Cretaceous-early Paleogene remains of seven genera attributed to the eurypterygian clade Aulopiformes (lizardfishes), a group for which detailed cladistic character sets describing patterns of variation in the branchial skeleton are available. We evaluate the placement of these fossil taxa based on characters of the gill skeleton in isolation. Our results support an alepisauroid placement for †*Apateodus corneti,* †*Cimolichthys lewesiensis* and †*Halec eupterygius*, and a stem synodontid affinity for †*Argillichthys toombsi* and †*Labrophagus esocinus*. These placements are broadly consistent with past hypotheses based either on formal cladistic argumentation or qualitative morphological comparison drawing on other skeletal systems. We find insufficient evidence in the branchial skeleton to place †*Aulopopsis depressifrons* more specifically than Aulopiformes *incertae sedis*. Gill-arch anatomy substantially revises past interpretations of †*Sardinioides illustrans* by providing clear evidence for placement within Aulopiformes generally, and as either a stem aulopid or stem paralopid more specifically. This species must therefore be removed from †*Sardinioides*, the type of which is a myctophiform and shows conspicuous anatomical differences with †'*S.*' *illustrans*. Our work provides proof-of-concept for the recovery of detailed information on gill skeleton anatomy in fossils, indicating the potential for the extraction of considerable new morphological data—and phylogenetic information—from suitably preserved fossil specimens.

45 KEY WORDS: Aulopiformes; computed tomography; Eurypterygii; gill skeletons; Teleostei.

46

Introduction

Owing to the large number of—and complex relationships between—their constituent bones and cartilages, gill skeletons represent a key source of morphological characters for inferring relationships among fishes (e.g. Nelson 1969; Rosen 1973; Wiley and Johnson 2010). Despite their prominence in studies of modern species, gill skeletons of fossil fishes remain an underutilized resource in phylogenetic datasets. Although mineralized components of gill arches can be readily preserved in the fossil record, they are known in detail for only a limited number of extinct taxa. Osteichthyan gill skeletons are obscured by overlying ossifications of the operculogular series, and the complex spatial relationships among their individual bones can be obliterated in heavily flattened specimens. The best-known gill skeletons in extinct fishes derive from specimens subjected to some kind of destructive analysis: serial grinding, which permits reconstruction of skeletal components and their positional relationships but results in destruction of the original sample (e.g. the tetrapodomorph sarcopterygian †*Eusthenopteron*: Jarvik 1980; the 'palaeoniscid' actinopterygian †*Pteronisculus*: Nielsen 1942); acid-transfer preparation, which liberates individual bones from surrounding matrix but obliterates their exact spatial relationships (e.g. the 'palaeoniscid' actinopterygians †*Mimipiscis* and †*Gogosardina*: Gardiner 1984, Choo et al. 2009; the Cretaceous teleost †*Aulolepis*: Patterson 1964) and acid- or mechanical-etching, which removes bone but leaves an impression (mould) from which positive models can be made using a flexible casting compound (e.g. the placoderm †*Jagorina*: Stensiö 1969; the acanthodian †*Acanthodes*: Miles 1973).

Micro computed tomography (μCT) permits internal study of specimens in a non-destructive manner, preserving the positional information of concealed bones. Where gill

skeletons are preserved they are often *in situ*, and considerable anatomical information can be extracted from them, as shown by recent studies of Palaeozoic fishes (e.g. the chondrichthyan †*Ozarcus*: Pradel et al. 2014; the actinopterygian †*Raynerius*: Giles et al. 2015).

The most informative studies of gill arches, regardless of methods of preparation, are based upon rare, three-dimensionally preserved crania. By contrast, details of branchial arch anatomy are substantially more limited in the flattened skeletons that dominate the fossil record of fishes. As a consequence, most descriptions of gill-arch morphology in fossils fishes are based on single exceptional fossils, rather than surveys of structure across a sample of different taxa. Here we apply μCT scanning to study a collection of exceptionally preserved fossil skulls associated with Aulopiformes. This work has two goals. The first, and more general, of these is to determine whether gill-arch anatomy can be extracted from fossil specimens in sufficient detail to evaluate synapomorphies established on the basis of the study of living species, with the obvious caveat that data from paleontological material will largely pertain to mineralized structures rather than those components that persist as cartilages, except in cases where the form of cartilages is constrained by surrounding bones. The second, more specific, goal is to evaluate past systematic interpretations of the particular fossil taxa examined here on the basis of their branchial anatomy.

Aulopiformes (lizardfishes and their relatives) is a small order of euteleosts, containing around 261 species and having a worldwide distribution, with members found in deep sea, benthic, and shallow-water ecosystems (Nelson 2016; Davis 2010). Aulopiformes represents the monophyletic sister group of Ctenosquamata, the clade comprising Myctophiformes (lanternfishes) and Acanthomorpha (spiny-rayed fishes) (Rosen 1973; Johnson 1992; Near et al. 2012; Betancur-r et al. 2013). Historically, the

97 monophyly of extant Aulopiformes has been debated, with characters of the gill skeleton
98 playing a key role in this discussion (Rosen 1973; Johnson 1982; Johnson 1992).
99 Aulopiform monophyly, as well as patterns of interrelationships among the order's
100 constituent lineages, draw considerable support from aspects of gill-arch anatomy.
101 Branchial skeletons of fossil aulopiforms clearly bear relevant phylogenetic data
102 even when their anatomy is very poorly known, as shown by Rosen's (1973: pgs 442-
103 452; table 1; fig. 68) investigation of incomplete material belonging to a handful of
104 Cretaceous specimens in his monumental study of euteleost interrelationships. Gill-arch
105 anatomy might be particularly significant in determining the placement of extinct
106 aulopiform taxa, as traits pertaining to the branchial skeleton make up a large proportion
107 of morphological characters (ca. 25%) in matrix-based cladistic analyses of the group
108 (Baldwin & Johnson 1996; Sato & Nakabo 2002; Davis 2010).
109 The aulopiform body fossil record ostensibly extends to the Early Cretaceous (Gallo
110 & Coelho 2008; Fielitz & González Rodríguez 2010), but the majority of specimens are Late
111 Cretaceous or younger in age. Three-dimensional material is known from chalk and clay
112 deposits (Friedman et al. 2016: fig. 1), with the majority of taxa from lithographic limestones
113 (e.g. Forey et al. 2003) and shales (e.g. Khalloufi et al. 2010) known only from flattened
114 specimens. Despite a rich record of articulated specimens, few analyses have attempted to
115 frame the relationships of fossil aulopiforms relative to living members of the group
116 (although see unpublished thesis by Silva 2011). Indeed, the few explicit associations of
117 fossil aulopiforms with either the group as a whole or its constituent clades are typically
118 based on a small set of traits dominated by dental features (e.g. Fielitz and Gonzáles
119 Rodríguez 2008). Here we build on this past work, with an emphasis on three-
120 dimensionally preserved material from the Late Cretaceous Chalk Group and Eocene
121 London Clay Formation of the United Kingdom (Fig. 1).

Material and methods

Institutional Abbreviations and Dagger Symbol

CAMSM, Sedgwick Museum, University of Cambridge, Cambridge, United Kingdom; NHMUK, Natural History Museum, London, United Kingdom; NBC RGM, Naturalis Biodiversity Centre, Leiden, the Netherlands.

Following Patterson and Rosen (1977), the names of extinct taxa are preceded with a dagger symbol ('†').

Materials

Seven specimens were investigated for inclusion in this study; †*Apateodus corneti* NBC RGM 446950, †*Argillichthys toombsi* NHMUK PV P49519, †*Aulopopsis depressifrons* NHMUK PV P26712, †*Cimolicthys lewesiensis* NHMUK PV P5491, †*Halec eupterygius* NHMUK PV P5662, †*Labrophagus escoinus* CAMSM TN 4286, and †*Sardinioides illustrans* NHMUK PV P3977. With the exception of †*Apateodus corneti*, all specimens studied here (Fig. 1) derive from the London Clay or English Chalk. For a review of the geological context of both these sites see Friedman et al. (2016).

In addition to these specimens, we also scanned material of †*Apateodus striatus* (Woodward 1901) (NHMUK PV OR49821), †*Dercetis maximus* (Woodward 1902) (NHMUK PV OR 31075-82), †*Enchodus lewesiensis* (Mantell 1822) (NHMUK PV P5415) and †*Eurypholis pulchellus* (Woodward 1901) (NHMUK PV P1703) from the English Chalk Group. The gill skeleton is not visible our scans of †*Dercetis maximus* or †*Eurypholis pulchellus*, and is limited to a few unidentifiable rod-like bones in †*Apateodus*

147 *striatus* and †*Enchodus lewesiensis*. Consequently these taxa were not included in our study,
148 although Rosen (1973: p. 449, fig. 68) reported and figured upper pharyngeal dentition in
149 †*Enchodus major* (NHMUK PV P49504).
150 Many of the Cretaceous genera yielding detailed gill-arch anatomy in CT scans are
151 represented by additional specimens that were acid prepared by Goody (1969), who
152 omitted the branchial skeleton from his descriptions. These specimens are highly
153 fragmented, with elements of the gill arches often mixed with fragments of other skull
154 bones. We examined acid-prepared gill-arch material of †*Apateodus striatus*, BGS
155 GSM26241, †*Cimolichthys lewesiensis* NHMUK PV P1810a and NHMUK PV P1811,
156 and †*Halec eupterygius* NHMUK PV OR43392. †*Halec eupterygius* NHMUK PV
157 P36237 preserves small rod like bones that likely represent branchial arches, but lack
158 sufficient diagnostic features to permit reliable identification of individual bones. Our
159 motivation in examining these chemically prepared specimens was not to provide
160 detailed descriptions, but rather as a check on the reliability of our accounts of primary
161 specimens studied using μCT.
162
163 **Computed Tomography**
164 All specimens subjected to μCT scanning have historically been subjected to mechanical
165 preparation in order to reveal the outer bones of the skull. Fossils were scanned with a
166 Metris X-Tek HMX ST CT scanner in the Imaging and Analysis Centre of the Natural
167 History Museum, London. The scan parameters (filters, current, voltage) are given in
168 Supplementary Information Table 1.
169 Tomogram stacks were segmented using Mimics Materialise v.16.0-18.0 x64
170 (http://biomedical.materialise.com/mimics). Different localities have different
171 preservational styles that influence the methods of digital segmentation and the quality of

the models produced. Gill skeletons are typically located near the center of the fossils examined, in the region of lowest X-ray penetration. Automated thresholding techniques are difficult to use in such cases, so segmentation was carried out by manually by adding specified grey values and interpolating between slices. Matrix surrounding fossils from the English Chalk Group and Maastricht Formation is of lower density than that of the London Clay Formation, leading to better X-ray penetration and improved contrast that permits segmentation of individual bones by separating them from a global threshold. Specimens from the London Clay Formation also show varying degrees of pyritization of both bone and surrounding matrix (e.g. Beckett & Friedman 2016). Some bones are preserved as void spaces within the matrix for samples from all deposits surveyed. These air-filled spaces are easily separated from matrix.

High-resolution models produced in Mimics were exported as .ply files, then imported into Blender (blender.org) and rendered as two-dimensional images. Blender was also used to virtually dissect gill skeletons, particularly in cases where the elements of the gill skeleton strongly overlapped. Where possible, the gill skeleton was reassembled in a postulated life position on a single plane (with the dorsal gill skeleton rotated over, as in standard depictions of gill skeletons in living taxa).

Morphological Characters and Analysis

We used the synapomorphy scheme for living aulopiforms presented by Davis (2010; in turn modified from Baldwin & Johnson 1996 and Sato & Nakabo 2002) to interpret the placement of fossil specimens based on branchial-arch anatomy. We have taken an algorithmic approach to 'inserting' highly incomplete taxa (*sensu* Grande & Bemis 1998) into a well-supported phylogenetic framework specified *a priori*. We scored each of our fossil

197 specimens for the 32 of 139 morphological characters pertaining to the gill skeleton in
198 the data matrix of Davis (2010). We then applied the combined (i.e. morphology +
199 molecular) Bayesian tree given in that study (Davis 2010: fig. 8) as a backbone
200 topological constraint to evaluate the placement of each fossil individually via parsimony
201 analysis in PAUP* Version 4.0a152 for Mac (Swofford 2002). Non-aulopiforms
202 included in our analysis are *Polymixia japonica, Metavelifer multiradiatus,*
203 *Nannobrachium lineatum, Benthosema glaciale, Neoscopelus macrolepidotus,* and
204 *Diplophos taenia*. We excluded the remaining eight non-aulopiform (*Morone chrysops,*
205 *Oncorhynchus mykiss, Argentina sialis, Thaleichthys pacificus, Ijimaia antillarum,*
206 *Hiodon alosoides, Dorosoma cepedianum* and *Danio rerio*) included in Davis (2010)
207 because they are represented exclusively by molecular sequences in that dataset. The 32
208 characters used here are summarized in the Supplementary Information, and our
209 character-state assessments for our sample of fossils is given in Supplementary
210 Information Table 2.

211 Many gill-arch characters in our matrix, and in studies of teleost gill skeletons
212 more generally, relate in part or whole to the presence, size, or shape of cartilages rather
213 than bones. While cartilage and other soft tissue is rarely preserved in fossils, relevant
214 characters can sometimes be coded if the anatomy of the cartilage in question can be
215 constrained from the geometry of associated bones. For example, if the articular ends of
216 bones within articulated fossil gill skeletons are in close proximity, it is reasonable to
217 conclude that the intervening cartilages of these bones were themselves short. By
218 contrast, large gaps between such bones imply elongated cartilages. Using this approach,
219 we have been able to code characters 4 (articulation of pharyngobranchial 1 with either
220 the base or tip of the cartilage of epibranchial 1), 17 (degree of ossification of first
221 epibranchial and ceratobranchial) and 24 (elongation and degree of ossification of first

222 basibranchial). However, characters 2 (absence of a cartilaginous condyle on
223 pharyngobranchial 3 for articulation with epibranchial 2), 18 (presence of the so-called
224 'epibranchial 5', which is more properly considered an accessory element of
225 ceratobranchial 4; Carvalho et al. 2013), 21 (gap between fourth basibranchial cartilage
226 and fifth ceratobranchials), 22 (extension of third basibranchial relative to fourth
227 basibranchial cartilage) and 29 (ligament between first hypobranchial and ventral
228 hypohyal) cannot be coded from fossil material.
229
230 **Systematic Palaeontology**
231
232 **Teleostei** Müller, 1845
233 **Eurypterygii** Rosen, 1973
234 **Aulopiformes** Rosen, 1973
235 **Aulopoidei** Rosen, 1973 *sensu* Davis, 2010
236 **Synodontidae** Gill, 1862
237 †***Argillichthys*** Casier, 1966
238 †***Argillichthys toombsi*** Casier, 1966
239 **(Fig. 2)**
240
241 **Material**
242 NHMUK PV P49519 (holotype) is a three-dimensionally preserved skull from the
243 London Clay Formation (Eocene: Ypresian), Sheppey, UK. The gill arches are well
244 preserved in articulation.
245 **Description**
246 The gill skeleton is mostly intact (Fig. 2A) and preserves: the basihyal, basibranchials 1-

3, hypobranchials 1-3, ceratobranchials 1-5, epibranchials 1-4, pharyngobranchials 1-3 and upper pharyngeal toothplates 3 and 5. Components are largely in life position.

Basihyal, basibranchials and urohyal. The basihyal lies between the hypohyals at the anterior of the gill skeleton. It is a relatively small, flat bone that is disk shaped in dorsal view. Basibranchial 1 is a small pyramidal ossification in close articulation with basibranchial 2. Basibranchial 2 is elongate, and hourglass-shaped in ventral view. The dorsal surface of basibranchials 1 and 2 is completely covered by an elongate, hexagonal basihyal toothplate with a rough dorsal surface but no large teeth (Fig. 2B&D). Basibranchial 3 is widest anteriorly, with a narrow strut from the dorsal plane extending two thirds of the length of hypobranchial 3. The urohyal is rod-like anteriorly but flattens posteriorly to form a thin, dorsally-directed plate with a ridge on the ventral surface (Fig. 2B). This plate resembles a trapezoid in lateral view. The urohyal extends from basibranchial 2 to the anterior margin of ceratobranchial 5.

Hypobranchials and ceratobranchials. Hypobranchials 1 and 2 are long, rod-like bones, each bearing a ventromedial process marking its point of articulation with the basibranchials. Hypobranchial 2 is approximately two thirds of the length of hypobranchial 1. Hypobranchial 3 is half the length of hypobranchial 2. Hypobranchial 3 is narrow anteriorly and curves in the middle before widening to form a broad triangular plate posteriorly. Ceratobranchials 1 to 5 are straight rod-like bones, expanded anteriorly, with a groove on their ventral margins, they closely articulate with the hypobranchials separated by what is presumably a small cartilage. Ceratobranchial 5 bears a flat, ovoid toothplate that is covered with a scattering of small teeth.

Epibranchials. The long epibranchial 1 bears a groove on its dorsal margin that extends two-thirds of the length of the bone (Fig. 2C&E). An uncinate process extends from the dorsal surface of epibranchial 1 at the end of this groove. Epibranchials 2 and 3 are

similar in shape to one another but progressively smaller. Both bear uncinate processes that extend anterodorsally. The ventral surface of epibranchial 3 bears an area that appears raised and roughened, and might represent an associated toothplate. Epibranchial 4 is a similar shape to epibranchial 3, but differs in lacking an uncinate process. A break at the rear of the fossil truncates epibranchial 4 on the left side of the skull.

Pharyngobranchials. Pharyngobranchial 1 is small, flattened, and hourglass shaped. Its anterior end is wide, and the right bone has been rotated out of life position (Fig. 2E). It is positioned directly anterior to epibranchial 1. Pharyngobranchial 2 articulates with the anterior end of epibranchial 2 via a long uncinate process. Pharyngobranchial 2 lies between epibranchial 2 and pharyngobranchial 3. Pharyngobranchial 3 is rod-like anteriorly but widens and flattens posteriorly where it supports a broad toothplate. On the left hand side of the specimen the posterior margin of pharyngobranchial 3 and its pharyngeal toothplate are closely associated with the anterior margin of the fourth upper pharyngeal toothplate. A broad bone on the right side of the specimen shows a similar morphology, and might represent a displaced fourth upper pharyngeal toothplate. It bears a rough ventral surface, which we interpret as the remains of teeth. A small, nodular ossification on the right-hand side of the dorsal gill skeleton, which is truncated by the posterior margin of the fossil, likely represents a fragment of upper phyarngeal toothplate 5. Truncation of the rear of the fossil is more anteriorly located on the left side of the skull, and we can detect no remains of pharyngeal toothplate 5.

†*Labrophagus* Casier, 1966

†*Labrophagus esocinus* Casier, 1966

(Fig. 3)

Material

297 CAMSM TN 4286 is a three-dimensionally preserved skull from the London Clay
298 Formation (Eocene: Ypresian), Sheppey, UK. The arches are well preserved in
299 articulation. However, contrast near the centre of this large specimen is poor in
300 tomograms, making some details of the arches unclear.

301 **Description**

302 The gill skeleton (Fig. 3A) preserves: the basihyal toothplate, basibranchials 1-2,
303 hypobranchials 1-3, ceratobranchials 1-5, epibranchials 1- 3, and pharyngobranchials 1-
304 2. Some bones are difficult to reconstruct due to low contrast in tomograms, but their
305 general structure and relationships are visible.

306 **Basihyal, basibranchials and urohyal.** The large, ovoid basihyal toothplate is inclined
307 anteriorly. Basibranchial 1 is a small, pyramid-shaped bone closely associated with
308 basibranchial 2. Basibranchial 2 is a long hourglass-shaped element with a toothplate on
309 the dorsal surface (Fig. 3B&E). The toothplate is elongate, with an expanded anterior
310 portion, and overlaps the posterior margin of basibranchial 1. Basibranchial 3 lies
311 posterior to basibranchial 2, but is not well resolved in scans. It is a small, pyramidal
312 bone. The urohyal has been rotated from life position. It is 'T'-shaped when viewed in
313 cross section, with an expanded plate extending latero-ventrally between hypobranchial 3
314 and the ceratobranchials.

315 **Hypobranchials and ceratobranchials.** Hypobranchials 1 and 2 are long ossifications
316 that widen anteriorly and bear a medio-ventral protrusion for articulation with the
317 basibranchial (Fig. 3B&E). Hypobranchial 2 is approximately two thirds of the length of
318 hypobranchial 1. Hypobranchial 3 is half the length of hypobranchial 2, and is only
319 preserved on the left side of the gill skeleton. Hypobranchial 3 consists of a thin strut of
320 bone anteriorly which widens posteriorly to form a thick 'v'-shaped plate.
321 Ceratobranchials 1 to 5 are rod-like bones that associate closely with the hypobranchials.

With the exception of ceratobranchial 3, which is slightly curved anterio-medially, they are straight bones. The ceratobranchials are slightly wider anteriorly and bear a longitudinal groove on their ventral surface. Only the posterior of ceratobranchial 1 is preserved on the left side, and has been displaced beneath ceratobranchial 2. Ceratobranchial 5 has a medial expansion that is connected to the rest of the bone by a narrow base. It is possible that the resulting gap would be covered in a thin lamina of bone which is not resolved in tomograms. Teeth are scattered on the medial margin of the anterior half of ceratobranchial 5, as well as along the medial extension.

Epibranchials. Epibranchial 1 is a long bone with a dorsal groove extending anteriorly as far as the dorsally-directed uncinate process (Fig. 3C&F). Epibranchial 2 is two-thirds the length of epibranchial 1 and widens anteriorly and posteriorly. On its antero-dorsal surface it bears a small uncinate process (Fig. 3F). Epibranchial 3 is slightly shorter than epibranchial 2 and has a groove on its dorsal margin. A protrusion visible on the right epibranchial 3 might represent an uncinate process, although this interpretation is not definitive.

Pharyngobranchials. A small, triangular bone on the left side of the fossil may represent either pharyngobranchial 1 or the anterior end of ceratobranchial 1. Pharyngobranchial 2 is hourglass shaped, with a large posterior expansion (Fig. 3D&G). A narrow process extends from the constricted part of the bone. Pharyngobranchial 2 articulates with the base of the uncinate process of epibranchial 1. More posterior pharyngobranchials or associated toothplates are not visible in our scans.

Alepisauroidei *sensu* Davis, 2010

†Ichthyotringidae Jordan, 1905

†***Apateodus*** Woodward, 1901

347 †***Apateodus corneti*** (Forir, 1887)

348 **(Fig. 4)**

349 **Material**

350 NBC RGM 446950 is a three-dimensionally preserved skull from the Maastricht
351 Formation, (Late Cretaceous: Maastrichtian, 67.6-66.0 Ma (Kruizinga 1924; J. Jagt pers.
352 comm. January 2017), Limburg, the Netherlands. The external anatomy of this specimen is
353 described by Kruzinga (1924) and additional details of the depositional setting are given by
354 Jagt & Jagt-Yazykova (2012). The specimen preserves an almost complete gill skeleton in
355 life position, largely in articulation.
356 For comparative purposes, we also examined an acid-prepared specimen of a different
357 species of *Apateodus*: *A. striatus* BGS GSM 26241 from the Cenomanian of the English
358 Chalk group. Observations are included below in the 'Remarks' section. Although Goody
359 (1969) provided a complete description of the skull of this individual, he did not present any
360 details of the branchial skeleton.

361 **Description**

362 The gill skeleton comprises the basihyal, basibranchials 1-4, hypobranchials 1-3,
363 ceratobranchials 1-3 and 5 (ceratobranchial 4 is not preserved, and may have been
364 cartilaginous), epibranchials 1-3, and pharyngobranchials 2 and 3. A poorly resolved
365 fragment of the posterior gill skeleton might represent either epibranchial 4 or part of an
366 upper pharyngeal toothplate. The urohyal is not preserved.

367 **Basihyal, basibranchials and urohyal.** The basihyal articulates with the two dorsal
368 hypohyals at the midline. It is a small conical bone, and slightly wider anteriorly than
369 posteriorly. There is no distinct basihyal toothplate, although it may be so intimately
370 fused to the basihyal that the division between these bones cannot be resolved in
371 available tomograms. The first basibranchial is the same shape and size as the basihyal. It

closely articulates with the basihyal anteriorly and the second basibranchial posteriorly. Basibranchial 2 is long and triangular in medial view, and curves down either side of the midline to form a gutter ventrally. The anterior region of basibranchial 3 resembles that of basibranchial 1. However, basibranchial 3 is greatly extended posteriorly, making it roughly twice the length of basibranchial 1. A narrow toothplate sits above, but is not tightly connected to, basibranchials 2 and 3. It extends anteriorly over basibranchial 1 and posteriorly over basibranchial 3. The toothplate bears no obvious tooth sockets or large teeth, but instead has a rough surface suggesting that it was covered with a field of small denticles.

Hypobranchials and ceratobranchials. The hypobranchials decrease in size from hypobranchial 1 to hypobranchial 3, and each member of this series articulates proximally with the basibranchial series (Fig. 4A). Hypobranchial 1 is rod-like and bears a small medial protrusion where it articulates with the posterior surface of basibranchial 1. The expanded articular head of hypobranchial 2 joins the basibranchial series near the articulation of basibranchials 2 and 3. Hypobranchial 3 is short and triangular, with a small process on the mesial edge of the bone near its proximal end. Hypobranchial 3 articulates with basibranchial 4. Ceratobranchials 1-3 are long and thin (Fig. 4B&C), and are slightly expanded at both their proximal and distal ends. Each bears a prominent groove along its ventral surface, and none show any obvious evidence of gill rakers. A gap between ceratobranchials 3 and 5 was presumably occupied by ceratobranchial 4, which is not preserved and may have been cartilaginous. Ceratobranchial 5 is present and has a rounded anterior margin. It is difficult to assess relative length as the posterior edge is broken, but as preserved this bone is slightly shorter than ceratobranchial 3. The bone is gently curved and bears a single row of large, pointed teeth of approximately equal size on its medial margin. The more intact right ceratobranchial 5 bears at least 12 teeth

that are evenly spaced along the length of the bone.

Epibranchials. Epibranchial 1 is longer than epibranchial 2 and widens anteriorly. An uncinate process is borne on epibranchial 1 and lies adjacent to that of pharyngobranchial 2; it is probable that they articulated (Fig. 4D&E). Epibranchial 2 is approximately twice the length of epibranchial 3 and is rod-like with a gutter along its dorsal surface. The uncinate process of epibranchial 2 is present but closely applied to the main body of the bone (Fig. 4F&G). The "y"-shaped epibranchial 3 is preserved in articulation with ceratobranchial 3. The bone expands distal to this articulation with a modestly developed uncinate process, and bears a shallow longitudinal groove on its dorsal surface. A poorly resolved, plate-like ossification similar in shape to epibranchial 3 might represent epibranchial 4 or, alternatively, one of the posterior upper phyarngeal toothplates (see below).

Pharyngobranchials. Pharyngobranchial 1 is rod-shaped, and is applied to the underside of epibranchial 1 (Fig. 4E). It is possible that the bone is incompletely preserved or damaged, and is wholly absent in the right side of the specimen. Pharyngobranchial 2 is preserved on both sides and lies almost parallel to pharyngobranchial 3 and anterior to epibranchial 2. A prominent uncinate process issues from pharyngobranchial 2 at mid-length. Pharyngobranchial 3 is a relatively thin cylindrical bone that widens and flattens posteriorly to form a toothplate. It lies on the mesial side of epibranchial 2 and pharyngobranchial 2. Apart from the bone of uncertain identity lying behind epibranchial 3 on the left side of the specimen, we have been unable to observe any remains consistent with upper pharyngeal toothplates 4 or 5.

Remarks

Reasonably well-preserved, acid-prepared remains of the branchial skeleton are available for †*Apateodus striatus* BGS GSM 26241 (Fig. 5). The specimen is disarticulated, with

422 no record of positional information. This seriously compromises any attempt to identify
423 individual components of the gill skeleton. However, we can confidently identify the
424 urohyal (Fig. 5A), a basihyal toothplate (Fig. 5B), a right hypobranchial (Fig. 5C), a
425 series of more anterior ceratobranchials (Fig. 5D&F) and right and left ceratobranchial 5
426 (Fig. 5E). Less certain are portions of either epibranchial 1 or 2 (Fig. 5F), and left
427 epibranchial 3 and associated upper pharyngeal toothplate 4 (Fig. 5G). The urohyal,
428 which is missing in †*Apateodus corneti,* has a ventral shelf, with a dorsally projecting
429 plate. The anterior of the urohyal forms an articular head (Fig. 5A). The basihyal
430 toothplate, which is not apparent in †*A. corneti*, is wide posteriorly, tapering to a point
431 anteriorly (Fig. 5D). It bears small teeth covering its dorsal surface. One of the right
432 hypobranchials is preserved, likely hypobranchial 1 or 2 (Fig. 5C). It is wide anteriorly
433 with two heads for articulation with the basibranchials, and then bends and narrows
434 posterior to this head, before widening posteriorly. The posterior margin of the bone is
435 broken. Five straight, elongate bones with a groove on their ventral surface are also
436 preserved (Fig. 5D). These are likely ceratobranchials, but identification is uncertain due
437 to disarticulation. Two are attached to epibranchials by consolidant used during
438 preparation and could also be remnants of the dorsal gill arches (Fig. 5F). They bear no
439 obvious toothplates or rakers. Clearly identifiable are both toothplates of ceratobranchial
440 5 (Fig. 5E). In dorsal view these are wider anteriorly, forming a broad plate that narrows
441 posteriorly to a point where the bone is likely broken. The dentition of ceratobranchial 5
442 comprises a single lateral row of large teeth, with three rows of smaller teeth that extend
443 in series parallel to this larger set. From the dorsal gill arches, either epibranchial 1 or 2
444 is preserved from both sides of the specimen. The anterior portion of the right side, and
445 the whole of the left side. The bone bears a small uncinate process (Fig. 5E) that is very
446 similar in shape and length to †*A. corneti.* Unfortunately it is not possible to identify

whether this is epibranchial 1 or 2 as the bones are no longer in articulation. Additionally, the bone from the left side is adhered to other bones by a consolidant. A small bone (Fig. 5G) that widens posteriorly and bears a toothplate anteriorly may be the left epibranchial 3 with the associated upper pharyngeal toothplate 4. The toothplate is round and covered with small teeth on its ventral surface.

†Cimolichthyidae Goody, 1969

†Cimolichthys Leidy, 1857

†Cimolichthys lewesiensis Leidy, 1857

(Fig. 6)

Material

NHMUK PV P5491 is a three-dimensionally preserved skull from the English Chalk Group, Lewes, Sussex, UK. It was likely collected from the traditional zones †*H. subglobosus* to †*T. gracilis* (Woodward 1902), which corresponds to the latest Cenomanian and early Turonian (Friedman et al. 2016). This specimen preserves only a partial gill skeleton, and it is clear that this structure was damaged and largely lost due to historical preparation. Two specimens of †*Cimolichthys* were acid prepared by Goody (1969): NHMUK PV P1811 and NHMUK PV P1810a. NHMUK PV P1811 was collected from an unknown locality, presumably located in southern England. The age of the specimen cannot be determined but key collecting localities of southern England are Cenomanian to Turonian in age (Friedman et al. 2016). NHMUK PV P1810a was originally collected from the English Chalk Group, Kent, UK and most likely comes from the traditional zones †*H. subglobosus* to †*H. planus* (Woodward 1902), which corresponds to the Cenomanian to Turonian (Friedman et al. 2016).

Description

The gill skeleton of NHMUK PV P5491 has been displaced toward the underside of the neurocranium due to dorsoventral compression of skull. Most of the gill skeleton has been severely damaged or destroyed by historical preparation, and only fragments remain. Hypobranchials 1-3 and ceratobranchials 2-3 are preserved on both sides, with ceratobranchial 1 preserved on the right side only. The basihyal and basibranchials 1-3, along with their associated toothplates, are also preserved. Fragmentary components of the dorsal gill skeleton are present, but are too incomplete to interpret.

In terms of gill-arch structures, NHMUK PV P1810a is the more complete of the two acid-prepared specimens although it is still fragmentary and disarticulated. NHMUK PV P1810a preserves: the urohyal, basibranchials 2-3, hypobranchials 1-3 from both sides, a number of ceratobranchials including ceratobranchial 5, and elements of the dorsal gill arches, some of which bear teeth. The less complete specimen NHMUK PV P1810a was cast before preparation, and this copy clearly shows that fragments of the gill skeleton were present prior to acid preparation. However, disarticulation and fragmentation occurring during preparation leaves only three bones identifiable as from the branchial arches: two hypobranchials, still partially embedded in Chalk and each with a large anterior articular head, and a probable fragment of ceratobranchial 5. These specimens are referenced below where they preserves bones that cannot be observed in the individual examined using μCT.

Basihyal, basibranchials and urohyal. The basihyal toothplate is an elongate plate-like bone, with a deep anterior notch. Teeth are carried on the bone either side of the notch and oppose a single row of large teeth on the vomer. Although teeth are present on the right side of the basihyal, only sockets remain on the left. The hypohyals articulate with the anterior end of the hourglass-shaped basibranchial 1, which is elongate and

497 overlapped posteriorly by basibranchial 2. Hypobranchial 1 articulates with the mid-
498 posterior region of basibranchial 1. Basibranchial 2 is an elongate flat bone that is
499 narrower posteriorly than anteriorly and bears a toothplate on its dorsal surface.
500 NHMUK PV P1810a, shows that this toothplate bears wings that extend down the lateral
501 surfaces of basibranchial 2. Basibranchial 3 is elongate, with a small ridge posteriorly
502 where it articulates with the second hypobranchials. The urohyal is fragementary, broken
503 anteriorly and dorsally, and is preserved as a straight bone with a broken dorsal
504 expansion (Fig. 6C).
505 **Hypobranchials and ceratobranchials.** Most of the hypobranchials are present only as
506 fragments. The anterior portion of hypobranchial 1 is preserved on both sides.
507 Hypobranchial 2 is present on the left side only. A triangular bone, closely associated
508 with basibranchial 3, is interpreted as hypobranchial 3. In NHMUK PV P1810
509 hypobranchial 3 is preserved on both sides of the specimen. On the right side the bone is
510 broken anteriorly and resembles the broken hypobranchial of NHMUK PV P5492. On
511 the left side hypobranchial 3 is hourglass shaped, wider posteriorly and narrowing
512 anteriorly as it twists mesially. The hypobranchials appear to have been straight bones,
513 decreasing in size from hypobranchial 1 to hypobranchial 3. The ceratobranchials are
514 straight, rod-like bones, with a deep longitudinal groove on their ventral surface.
515 Ceratobranchial 1 is preserved on the left, although the posterior portion is missing, and
516 both ceratobranchials 1 and 2 are preserved on the right. Ceratobranchial 1 and 2 are
517 similar in shape, although ceratobranchial 2 is more strongly curved. There are no
518 obvious gill rakers. Both acid prepared specimens preserve fragments of ceratobranchial
519 5. It bears an outer row of large teeth with one (NHMUK PV P1810a) to two (NHMUK
520 PV P1811) rows of smaller teeth medially (Fig. 6D). There is a mesial expansion from
521 the tooth-bearing shelf.

Remaining bones in NHMUK PV P5491 are unidentifiable, but are likely part of the dorsal gill skeleton. Although we have not observed them in our fossil due to historical preparation, Rosen (1973: p. 449) reported upper pharyngeal dentition in another specimen of †*Cimolichthys* from the English Chalk Group (NHMUK PV P10746) comprising narrow upper pharyngeal toothplates 3 and 4, with the former fused to the endoskeleton.

†Halecidae Agassiz, 1834

†*Halec* Agassiz, 1834

†*Halec eupterygius* Dixon, 1850

(Fig. 7)

Material

NHMUK PV P5662 is a three-dimensionally preserved skull collected from a Turonian zone (Woodward 1902) of the English Chalk Group, Maidstone, Kent, UK.

NHMUK PV OR 43392 is an acid prepared specimen that was listed in Woodward (1901; p. 218) as "Small cranium and part of jaws; English Chalk". There is no locality or age data associated with this specimen but it is likely to be Cenomanian orTuronian in age (Friedman et al. 2016).

Description

The gill skeleton of *Halec* is almost completely preserved in NHMUK PV P5662, although the posterior regions of some bones are lost due to truncation of the fossil. Unfortunately, it is almost impossible to identify bones in the positions in which they are preserved due to the narrow skull of *Halec*, which appears to at least partially reflect genuine anatomy rather than taphonomic distortion. Virtual dissection of the specimen permits tentative identification of some bones and reconstruction of a hypothesised life

547 arrangement. However, beyond pairing right and left bones, it is difficult to identify the
548 arch to which individual components belong.
549 Acid-prepared specimen NHMUK PV OR 43392 (Fig. 7K-L) preserves the left
550 and right gill arches in articulation. However the posterior half of the gill arches is
551 incomplete along a plane, presumably indicating that the posterior part of the skull was
552 broken prior to chemical treatment. The specimen preserves basibranchial 2,
553 hypobranchials 1-2, ceratobranchials 1-5 and the urohyal.
554 **Basihyal, basibranchials and urohyal.** The basihyal is missing in both specimens.
555 Basibranchial 1 is small and sits between the anterior projection of the ceratohyals,
556 Basibranchial 2 is short, with a toothplate sutured to its dorsal margin. The toothplate is
557 hourglass-shaped in dorsal view, and extends far beyond the anterior and posterior
558 margins of basibranchial 2. The toothplate bears wings that extend down the lateral
559 surfaces of basibranchial 2. The urohyal comprises a dorsal rod bearing two laterally
560 developed wings, giving the bone a "v"-shape (Fig. 7F-G&J)
561 **Hypobranchials and ceratobranchials.** Hypobranchials 1 and 2 bear ventrally directed
562 processes that articulate with the basibranchials (Fig. 7J). Ceratobranchials 1-5 are
563 arranged in approximate life position (Fig. 7B-C,G&J). Ceratobranchials 1-4 are straight
564 rod-like bones with no obvious gill rakers. Ceratobranchial 5 is an expanded plate-like
565 bone. In NHMUK PV P5662 a single row of large teeth is visible running down the
566 medial edge of its dorsal surface (Fig. 7C). It bears between 12 (on the right) and 16 (on
567 the left) sockets, with one tooth preserved on the right and 5 on the left. In NHMUK PV
568 OR 43392 (Fig. 7K-L) only the anterior tip of ceratobranchials 5 are preserved. They
569 bear a single large row of teeth on the mesial margin with multiple rows of smaller teeth
570 laterally.
571 **Epibranchials.** The dorsal gill skeleton is more difficult to interpret than ventral

components. Identification of epibranchial 2 is not possible, and hence the condition of any uncinate process cannot be directly assessed, although none of the preserved epibranchials bears an enlarged uncinate process (Fig. 7D-E,H-I). However, these bones are weakly ossified, raising the possibility that such structures might not be preserved in *Halec*.

Pharyngobranchials. Some rod-like ossifications present in the dorsal gill skeleton of *Halec* might represent pharyngobranchials or associated toothplates, but it is not possible to make identifications with confidence.

Aulopiformes *incertae sedis*

†***Aulopopsis*** Casier, 1966

†***Aulopopsis depressifrons*** Casier, 1966

(Fig. 8)

Material

NHMUK PV P26712 (holotype), a three-dimensionally preserved skull, London Clay Formation (Eocene: Ypresian), Sheppey, UK. This specimen preserves an almost complete gill skeleton that is in partial articulation, making identification of some bones difficult.

Description

Components of both the dorsal and ventral gill skeleton are present. The dorsal gill skeleton is more severely displaced, but nevertheless shows epibranchials 1-3 and pharyngobranchials 1-3, with the left side being better preserved. The ventral gill skeleton preserves basibranchials 2 and 3, hypobranchials 1-3 and ceratobranchials 1-4. The urohyal is also preserved.

Basihyal, basibranchials and urohyal. Basibranchial 2 is medially constricted in dorsal

597 view, with an anterior and posterior head (Fig. 8B&D). The posterior head articulates
598 with the anterior of basibranchial 3. Basibranchial 3 is a relatively straight, elongate bone
599 that extends from the posterior of basibranchial 2 to half the length of the third
600 hypobranchial; it has a small expansion anteriorly for articulation with basibranchial 2.
601 The urohyal is straight anteriorly with a small anterior expansion (Fig. 8A). The posterior
602 of the urohyal is expanded as a plate-like structure, but is poorly preserved.
603 **Hypobranchials and ceratobranchials.** Hypobranchials 1 and 2 are long, straight bones
604 that bear a broad anterior expansion (Fig. 8B&D). Hypobranchial 2 is two-thirds the
605 length of hypobranchial 1, and articulates with the posterior of basibranchial 2.
606 Hypobranchial 3 is a triangular bone with an anterior rod-like projection for articulation
607 with basibranchial 3. Ceratobranchials 1 to 4 are preserved on both sides of the gill
608 skeleton and closely associated with the hypobranchials suggesting a small intervening
609 cartilage head. They are straight, rod-like bones that broaden anteriorly and bear a
610 longitudinal groove on their ventral surface.
611 **Epibranchials.** Epibranchial 1 is the longest of the epibranchials (Fig. 8C&D). It bears a
612 groove on its dorsal surface and expands dorsally into an uncinate process. A fragment of
613 bone that aligns with the dorsal expansion may represent a second tubular extension,
614 which could be interpreted as either an uncinate process or a continuation of the bone,
615 although poor contrast in tomograms makes this difficult to determine. Epibranchial 2 is
616 half the length of epibranchial 1, curves laterally, is grooved dorsally, and bears an
617 elongate uncinate process. Epibranchial 3 is slightly shorter than epibranchial 2, is also
618 curved and has a shallow groove on its dorsal surface. However, it lacks an uncinate
619 process.
620 **Pharyngobranchials.** Pharyngobranchial 1 is a small, medially constricted bone that
621 widens posteriorly (Fig. 8C&D). Pharyngobranchial 2 is a curved bone which is flattened

posteriorly and forms a head anteriorly. The bone bears a small posteriorly directed process at midlength. Pharyngobranchial 3 is straight, and is slightly expanded towards the posterior of the bone. We cannot detect any of the dorsal pharyngeal toothplates, due to disruption to the dorsal gill skeleton.

†*Sardinioides* von der Marck, 1858

†*Sardinioides illustrans* Woodward, 1902

(Fig. 9)

Material

NHMUK PV P3977 (holotype), three-dimensionally preserved skull and most of the postcranial skeleton (caudal skeleton missing), English Chalk Group (Late Cretaceous: Cenomanian-Turonian). Woodward (1902) described its locality and horizon as "Unknown – but probably from one of the lower zones in the Burham district, Kent" (Woodward 1902: p. 35), although the associated label specifies the collection locality as Sussex, UK. If the specimen derives from the lower part of Blue Bell Hill, Kent, then it would correspond to the traditional zones *H.subglobosus* to *T. gracilis* (latest Cenomanian to early Turonian); if from Lewes, Sussex it has a broader age range, from the mid-Cenomanian to earliest Turonian (Friedman et al. 2016).

Description

The dorsal part of the gill skeleton is articulated and almost complete: epibranchials 1-4, pharyngobranchials 2-3 and upper pharyngeal toothplates 3-5 are all present. However, only parts of the right hand side of the ventral gill skeleton are preserved: the basihyal toothplate, basibranchial 2, hypobranchials 1-2, ceratobranchials 1-5. Identities of some elements cannot be determined, but these are most likely from the ventral gill skeleton.

Basihyal, basibranchials and urohyal. Basibranchial 2 is a long hourglass-shaped bone

(Fig. 9A,B&C). It has an associated toothplate that tapers to a point at either end. The urohyal is a broad flat plate with a thickened ridge along the ventral margin and is approximately triangular in lateral view. It is poorly resolved posteriorly, suggesting the bone is weakly mineralized.

Hypobranchials and ceratobranchials. Hypobranchials 1 and 2 are long, straight bones (Fig. 9B&D). Hypobranchial 1 is preserved best on the left side, with a broken anterior portion of hypobranchial 1 preserved on the right. Both hypobranchials 1 and 2 broaden anteriorly and bear a longitudinal groove ventrally. Hypobranchial 2 is shorter than hypobranchial 1. Ceratobranchial 1 is rotated 90 degrees from life position, but still clearly articulates closely with epibranchial 1 and hypobranchial 1 with a small cartilage. It is a long rod-like bone with a ventral groove. It curves posteriorly to articulate with hypobranchial 1. Ceratobranchials 2-4 are long rod-like bones, each with a groove on their ventral surface, and are best preserved on the right hand side of the fossil. Ceratobranchial 5 is the same length but expanded mesially to form an ovoid plate. The dorsal surface of the bone is rough but has no large teeth, suggesting it was covered with small denticles at or near the limit of the resolution of the scans.

Epibranchials. The dorsal gill skeleton is preserved in articulation on the right side of the specimen; descriptions in this section and the following one are based on this side of the fossil (Fig. 9C&E). Epibranchials 1 and 2 are long, rod-like bones that bear uncinate processes anteriorly. The uncinate process of epibranchial 1 articulates with the anteriorly placed uncinate process of pharyngobranchial 2. Epibranchial 2 is a long bone with two articular heads. The anterior head articulates with the posterior tip of pharyngobranchial 2, and the lateral with pharyngobranchial 3. Epibranchial 3 is a short bone with an uncinate process that articulates with the ‘Y’-shaped epibranchial 4. Epibranchial 4 narrows posteriorly, and is forked anteriorly, marking articulations with epibranchial 3

672 and the dorsal surface of the fourth pharyngeal toothplate, where presumably a
673 cartilaginous pharyngobranchial 4 would lie.
674 **Pharyngobranchials.** Pharyngobranchial 2 is a small bone with a dorsally directed
675 uncinate process (Fig. 9C&E). Pharyngobranchial 3 is teardrop shaped, with a tapered
676 anterior end and wide posterior end, and bears a facet halfway along its mesial margin
677 for articulation with epibranchial 2. Pharyngobranchial 3 bears a ridge extending
678 anteroposteriorly on the mesio-dorsal margin, and bears a broad toothplate covered with
679 denticles on on its ventral surface. Pharyngobranchial 3 articulates postero-laterally with
680 the anterior tip of epibranchial 3. Upper pharyngeal toothplate 4, a circular ossification
681 covered in small teeth in ventral view, is associated with the posterior margin of upper
682 pharyngeal toothplate 3. Posterior to this, on the ventral surface of epibranchial 4, is
683 upper pharyngeal toothplate 5. This is of similar shape and size to upper pharyngeal
684 toothplate 4.
685
686 **Discussion**
687
688 Aulopiform monophyly is supported by numerous anatomical synapomorphies (seven:
689 Wiley and Johnson 2010; nine: Davis 2010). As most morphological analyses of
690 aulopiforms focus exclusively on extant taxa (Baldwin & Johnson 1996; Sato & Nakabo
691 2002; Davis 2010), many of these characters pertain to features not preserved or easily
692 observed in fossils. Baldwin & Johnson (1996) identify seven derived features
693 supporting the monophyly of aulopiformes, of which four are potentially checkable in
694 fossils: an elongate uncinate process on the second epibranchial (Rosen 1973), the
695 epipleural series extending anteriorly to at least vertebra 2 (Patterson & Johnson 1995),
696 displacement of one or more of the anterior epipleurals dorsally into the horizontal

697 septum (Patterson & Johnson 1995) and fusion of the medial processes of the pelvic
698 girdle. These characters are upheld in the synthetic review of the literature by Wiley and
699 Johnson (2010). Sato & Nakabo (2002) report an additional synapomorphy of the order:
700 palatine not expanded laterally. Davis (2010: p. 433-4) reiterates these characters, but
701 reports an additional putative synapomorphy: presence of a 'fifth epibranchial'
702 (accessory element of ceratobranchial 4; Carvahlo et al. 2013). We regard this
703 optimization as spurious as it stems from a restricted morphological outgroup comprising
704 mycophiforms and early diverging acanthomorph lineages (which lack the accessory
705 element of ceratobranchial 4) and the stomiiform *Diplophos* (which is coded as
706 uncertain; Fink & Weitzmann 1982 do not describe or illustrate the element in
707 *Diplophos*, but a miniscule cartilage is reported by Baldwin & Johnson 1996, p. 372).
708 Instead, an accessory element of ceratobranchial 5 is widely distributed in teleosts, likely
709 present in the last common ancestor of the crown (Carvalho et al. 2013: fig. 8). We
710 therefore regard the presence of an accessory element of ceratobranchial 5 in aulopiforms
711 as retention of a general condition rather than a feature uniting the clade. A series of
712 additional gill skeleton features support the monophyly of clades nested within
713 Aulopiformes (Fig. 10). Here, we use the Bayesian total evidence topology presented by
714 Davis (2010; fig. 7) to evaluate the possible positions of fossil aulopiforms described
715 based on structure of their gill skeletons (reconstructions shown in Fig. 11).
716
717 **Using gill skeletons to place fossils**
718 Past placements of the fossils examined here have principally been based on verbal
719 argumentation (e.g. Woodward 1902, Goody 1969, Rosen 1973). The few formal
720 cladistic analyses conducted are generally concerned with fossils, with limited sampling
721 of living aulopiform species (Fielitz & Gonzalez Rodriguez 2008, Silva & Gallo 2011;

but see Fielitz 2004, Fielitz & Gonzalez Rodriguez 2010). Cretaceous taxa examined apart from †*Sardinioides* (i.e. †*Apateodus*, †*Cimolichthys*, †*Halec*) have broadly similar taxonomic histories that are summarized here. Remaining taxa are treated on a case-by-case basis in individual sections below.

Woodward (1901) placed †*Apateodus*, †*Cimolichthys*, and †*Halec* in his Enchodontidae, an assemblage of Cretaceous, fang-bearing taxa that he associated with modern alepisaurids (lancetfishes), evermannellids (sabretooths; Woodward's "Odontostomidae"), and 'scopelids' (a polyphyletic assemblage of aulopiform and myctophiform species). Goody (1969) divided Woodward's Enchodontidae into four groups that he recognized as suborders: Ichthyotringoidei (containing †*Apateodus*, among others), Cimolichthyoidei (containing †*Cimolichthys*, among others), Enchodontoidei (containing †*Enchodus* and several other taxa not studied here), Halecoidei (containing †*Halec*, among others). These fossil groups were arrayed as a grade outside of a clade corresponding broadly to Euteleostei of modern usage, minus Esociformes (pikes and mudminnows), in a hand-drawn phylogeny (Goody 1966: fig. 102). Rosen's (1973) analysis of euteleostean relationships represented the first attempt to discern the relationships of these Cretaceous fossils using explicit cladistic argumentation. He arrived at a series of key conclusions concerning the assemblage he termed 'enchodontoids', corresponding to Woodward's Enchodontidae, and thus an amalgam of Goody's Ichthyotringoidei, Cimolichthyoidei, Enchodontidae, and Halecoidei. First, that these Cretaceous fossils were aulopiforms generally, and alepisauroids specifically (comprising only paralepidids and alepisaurids of modern usage, rather than the more extensive meaning of the term adopted by Davis 2010, and applied here). Second, that this Cretaceous assemblage was unlikely to be monophyletic, with some being more closely related to extant alepisauroids than others. Subsequent

phylogenetic analyses incorporating some of these extinct forms have generally resolved them as a clade to the exclusion of living species, although their sampling of extant aulopiforms is generally limited (Fielitz 2004; Fielitz & Rodriguez 2010; Silva & Gallo 2011).

†Argillichthys toombsi. *†Argillichthys toombsi* is known from only one specimen, described by Casier (1966) and placed by him within Synodontidae (lizardfishes) based on the shape of the "cranial vault", the procumbent hyomandibula, and the structure of the teeth. None of these characters are diagnostic of Synodontidae or even Aulopiformes.

We were able to code *†Argillichthys* for 26 of 33 characters relating to the gill skeleton. This taxon shows an uncinate process on epibranchial 2 (1[1]) an aulopiform synapomorphy. Our constrained parsimony analysis of gill-arch characters places *†Argillichthys* as the sister lineage to all other synodontids. This placement is supported by the presence of some, but not all, derived features of the gill skeleton present in living members of that group. *†Argillichthys* shares with living synodontids an apparent absence of gill rakers (5[1]; also characteristic of Alepisauroidea) and the presence of ventrally directed processes on the first and second hypobranchials (30[1], 31[1]). However, other derived features of synodontids (Fig. 10), or of synodontid subclades, are not present. Characters conflicting with a stem synodontid placement include a pharyngobranchial 2 lacking an extra uncinate process but with an expanded proximal base (6[1]; present in Chlorophthalmidae), pharyngobranchial 2 with long uncinate process (8[1]), and absence of an uncinate process on epibranchial 4 (16 [3]). This final character is typical of Ipnopidae (deep-sea tripod fishes), but is also found in at least one taxon closely related to synodontids (*Pseudotrichonotus altivelis*; Johnson et al. 1996). We support Casier's initial interpretation of *†Argillichthys* as a synodontid, although not on the basis of the features he proposed (Fig.

772 12).

773

774 †***Labrophagus esocinus.*** †*Labrophagus esocinus* was studied by Casier (1966), who
775 noted its similarity to †*Aulopopsis* and placed the genus in Aulopidae on this basis; we
776 however regard †*Aulopopsis* as Aulopiformes *incertae sedis* (see above). We were able
777 to code 17 of 33 gill arch characters for †*Labrophagus*. The gill skeleton of
778 †*Labrophagus* bears an elongate uncinate process on epibranchial 2, confirming
779 placement within Aulopiformes. Our constrained cladistic analysis places †*Labrophagus*
780 as the sister lineage of Synodontidae. Characters relevant to this placement include the
781 apparent absence of gill rakers (5[1]; also present in Alepisauroidea) and the presence of a
782 ventrally directed process on hypobranchials 1 and 2 (30[1], 31[1]). Characters pertaining to
783 more derived members of Synodontidae are not present. There is, however, one character that
784 contradicts this hypothesis: the presence of a toothplate on the basibranchials (27[1]), which
785 is a derived character of Notosudidae within Aulopiformes. On the balance of available
786 evidence we conclude that †*Labrophagus* is a synodontid (Fig. 12), contradicting
787 Casier's original interpretation.

788

789 †***Apateodus corneti.*** †*Apateodus* is one of the oldest taxa associated with Aulopiformes,
790 with a fossil record extending into the Early Cretaceous (Albian; Newbrey & Konishi
791 2015). Association of †*Apateodus* with †*Apateopholis* and †*Ichthyotringa* as
792 ichthyotringoids, and their relative isolation from other 'Cretaceous alepisauroids'
793 *sensu* Rosen (1973), has been the conventional view since Goody (1969). Taverne
794 (2006) and Fielitz & Gonzalez Rodriguez (2008) question the association of these three
795 genera, arguing that the characters uniting them are plesiomorphic. However, the latter
796 present an analysis that recovers †*Apateodus* as sister to, or even nested within,

†*Ichthyotringa.* While published cladistic analyses include †*Apateodus* and other ichthyotringoids (Fielitz & Gonzalez Rodriguez 2008; Silva & Gallo 2011), these analyses do not test their position within Aulopiformes, or aulopiform affinity. An exception is Dietze (2009), who places †*Ichthyotringa* as an aulopiform among a neoteleost ingroup, in an analysis of 60 anatomical characters.

We have been able to code 22 of 33 gill-arch characters for †*Apateodus corneti*. Placement within Aulopiformes is justified by the presence of an uncinate process on the second epibranchial. However, this process assumes a distinctive morphology corresponding most closely to that of some paralepidids among living taxa (character 1[3]). Our constrained phylogenetic analysis places †*Apateodus corneti* within Paralepididae as the sister taxon of *Lestidium* on this basis (Fig. 12), although the precision of this placement is questionable. Interpretation as a paralepidid is further supported by the presence of a well-ossified first ceratobranchial and epibranchial (17[0]), although this represents a reversal. The absence of obvious gill rakers (5[1]) supports placement within Alepisauroidea, but is also found in synodontids. Characters conflicting with a paralepidid interpretation include an elongate second basibranchial (25[1]; characteristic of evermannellids) and the presence of a toothplate on basibranchial 2 (27[1]; characteristic of notosudids), which in the case of †*Apateodus* extends to cover basibranchials 1 and 3.

The fragmentary remains of †*Apateodus striatus* generally corroborate features apparent in †*A. corneti*. Most notable is the presence of a distinctive, paralepidid-like uncinate process on what might be the second epibranchial. The specimen also adds information on the structure of the urohyal, although no characters in our matrix pertain to this bone. The most conspicuous difference between these species of †*Apteodus* concerns the dentition of the fifth ceratobranchial. While both show a narrow area for

822 teeth rather than an expanded plate, †*A. striatus* bears several tooth rows while †*A.*
823 *corneti* appears to have only one. Minimally, this justifies separation of the English
824 Chalk and Maastrichtian †*Apateodus* at the specific level (cf. Kruzinga 1924, Friedman
825 2012), in contrast to Goody's (1969) inclusion of both in †*A. striatus*. We agree with
826 Newbrey & Konishi (2015) that the species of †*Apateodus* (Early Cretaceous: †*A.*
827 *glyphodus*; Late Cretaceous: †*A. busseni*, †*A. corneti*, †*A. striatus*) and the monotypic
828 †*Ursichthys* are closely related to one another, but an evaluation of their mutual relationships
829 is beyond the scope of the current study.
830
831 **†*Cimolichthys lewesiensis.*** Past phylogenetic interpretations of †*Cimolichthys*
832 broadly follow the outline provided for 'Cretaceous alepisauroids' above. In terms of
833 inclusion of living aulopiform taxa, Fielitz (2004) presented the most extensive cladistic
834 analysis to date that also sampled †*Cimolichthys*. He found †*Cimolichthys* as the sister
835 lineage of other echodontids, and that together these form a clade on the stem of
836 Alepisauridae.
837 We were only able to code 5 of 33 characters for the branchial skeleton of
838 †*Cimolichthys* from μCT data due to fragmentary preservation in the specimen studied. Two
839 additional characters were coded from acid prepared material. For all specimens, incomplete
840 preservation of the dorsal gill skeleton prevents the evaluation of potential synapomorphies of
841 Aulopiformes. Inclusion of †*Cimolichthys* in our constrained analysis places the genus with
842 Notosudidae, as either: sister to remaining notosudids, in a polytomy with remaining
843 notosudids, in a polytomy with *Scopelosaurus*, or as sister to *Scopelosaurus* (Fig. 12). This
844 placement is supported by the presence of elongate first and second basibranchials (24[1],
845 25[1]) and the presence of toothplates on the basibranchials (27[1]). Additional characters
846 gleaned from the acid prepared specimen does not change the placement of †*Cimolichthys*.

847 Thus we fail to corroborate an alepisauroid interpretation of †*Cimolichthys*, suggested by
848 other aspects of skeletal anatomy (Feilitz 2004). Although evidence from the gill skeleton is
849 scant a notosudid placement is recovered in this analysis.
850
851 †***Halec eupterygius.*** The phylogenetic history of †*Halec* matches that of other
852 'Cretaceous alepisauroids'. The most recent cladistic analysis to include †*Halec* places it
853 as the sister lineage to †*Phylactocephalus* (a halecoid *sensu* Goody, 1969; Silva & Gallo
854 2011). In turn, this pair represents the deepest diverging branch of a clade of taxa that
855 includes other enchodontoids *sensu* Rosen (1973). We were able to score †*Halec* for 8 of
856 33 gill arch characters. Our cladistics analysis consistently associates the genus with
857 Alepisauroidea, although its precise position is unclear. It is placed as: a stem member of that
858 group; a stem scopelarchid; the sister lineage of Evermannellidae + Sudidae + Alepisauridae
859 + Paralepididae; the sister lineage of Sudidae + Alepisauridae + Paralepididae; the sister
860 lineage of Evermannellidae; and nested within the Alepisauridae as a member of the clade
861 comprising *Omosudis* + *Alepisaurus* (Fig. 12). The latter five placements are supported by
862 the presence of teeth restricted to the medial edge of the fifth ceratobranchial (19[2]). The
863 acid prepared specimens also studied do not provide additional character information due to
864 the method of preparation and the characters under consideration. On the basis of the
865 character evidence from the computed tomography data, and evidence from other skeletal
866 systems, we are convinced that †*Halec* is a member of Alepisauroidea, but are uncertain of its
867 precise placement.
868
869 †***Aulopopsis depressifrons.*** †*Aulopopis depressifrons* was first described by Casier (1966),
870 who placed it in the Aulopidae due to perceived similarities in neurocranial anatomy with the
871 extant *Aulopus*. Casier distinguished †*Aulopopsis* from *Aulopus* by a "greater development of

872 the postorbital part of the cranial vault" (Casier 1966: p. 144; our translation from the
873 French). We have been able to code 13 of 33 characters for the gill skeleton of †*Aulopopsis*.
874 An aulopiform interpretation is supported by the presence of an elongate uncinate process on
875 epibranchial 2 (1[1]). The constrained cladistic analysis places †*Aulopopsis* with
876 Giganturoidae in one of three positions: sister to that clade as a whole, sister to *Gigantura*,
877 and sister to *Bathysaurus* + *Bathysauropsis*. However, this placement appears to be supported
878 principally on the inferred presence of toothplates rather than rakers on the gill arches, a
879 feature that occurs in several other aulopiform clades independently. Given the limited
880 character information available, we are hesitant to suggest such a precise placement for
881 †*Aulopopsis* on the basis of gill-arch anatomy alone. We conservatively regard this taxon as
882 Aulopiformes *incertae sedis*.
883
884 †***Sardinioides illustrans.*** The taxonomic history of †*Sardinioides* is complex. The type
885 species of the genus, †*S. monasterii*, is known from the Late Cretaceous (Campanian) of
886 western Germany. There are several additional referred species: †*S. crassicaudus* and †*S.*
887 *macropthalmus*, also from the Campanian of Germany (Goody 1969), †*S. frigoae* from the
888 latest Campanian-earliest Maastrichtian of Italy (Taverne 2008), and †*S. illustrans* from
889 older rocks of the southern UK and studied here (Rosen 1973: p. 456 dismisses Goody's
890 attribution of material from the Cenomanian of Lebanon to the genus). Early workers
891 related the species of †*Sardinioides* to 'scopelids', making comparison to taxa now
892 distributed between Aulopiformes and Myctophiformes. Rosen (1973) recognized that the
893 German examples of †*Sardinioides* (including the type species), shared a series of derived
894 features in common with mycophiforms, but that †*S. illustrans* appeared to be distinct from
895 these other stratigraphically younger species, and instead compared it with *Aulopus* (cf.
896 Woodward 1902: pl. 10) while still acknowledging a possible myctophiform affinity. The

German species of †*Sardinioides* have since been included in a cladistic analysis corroborating Rosen's (1973) hypothesis that they are, in fact, myctophiforms (Dietze 2009). Despite its completeness, †*S. illustrans* has not been subjected to any serious re-examination since Rosen (1973); we studied it in the hope that gill-arch anatomy might help to clarify its position relative to other species of †*Sardinioides* and higher teleosts more generally.

We are able to score 21 of 33 gill-arch features for †*S. illustrans*. Significantly, we find that the gill skeleton of †*S. illustrans* bears an uncinate process on the second epibranchial (1[1]), providing evidence for an aulopiform—rather than myctophiform—placement of the species. Ongoing work on this specimen reveals further information supportive of this interpretation: the presence of more than two branchiostegals articulating with the posterior ceratohyal, a primitive feature found in aulopiforms but not in ctenosquamates (Stiassny 1996), as well as fusion of the median pelvic processes and absence of the lateral expansion of the palatine, which represent aulopiform synapomorphies (Baldwin & Johnson 1996; Sato & Nakabo 2002).

Our constrained cladistic analysis resolves †'*S.*' *illustrans* as either a stem aulopid or stem paralopid (Fig. 12), and appears to reflect the generalized morphology of its gill skeleton. Despite some ambiguity in familial attribution, we are convinced by the evidence cited above that †'*S.*' *illustrans* is an aulopiform, and thus not attributable to the myctophiform †*Sardinioides*. A new genus will be required to accommodate this species, but is beyond the scope of the present study. We await more complete documentation of other aspects of its anatomy—as well as its phylogenetic position within Aulopiformes—before completing any such taxonomic revisions.

Limitations associated with the study of fossil gill skeletons

While our tomographic data for fossil aulopiforms provides new evidence for their phylogenetic placements, it is clear that the study of gill-arch anatomy in fossils using this approach does have limitations. These fall into three principal categories, which vary in terms of their relative severity. First, there are challenges associated with fossil specimens themselves, most notably in terms of degrees of distortion and disarticulation that are apparent even in exceptional, three-dimensionally preserved material like that targeted in this study. Distortion and incomplete preservation appears most severe in the dorsal gill skeleton, perhaps as a consequence of a smaller size of individual ossifications. Disruption, and the consequent loss of information on patterns of connections between bones, can make the assessment of the identity of specific components difficult. Additionally, most characters pertaining to cartilages of the gill skeleton cannot be coded in fossils, unless aspects of cartilage geometry can be inferred on the basis of ossified components. Second, it is clear that good comparative models are necessary for successful interpretation of partially disarticulated gill skeletons. This is clearly possible in the case of aulopiforms, where anatomy of living species has been described (e.g. Rosen 1973; Baldwin & Johnson 1996; Sato & Nakabo 2002) and can be further assessed via comparative material. Although gill-arch structure has been described in some fossil fishes without closely related living comparators (e.g. Nielsen 1942), we anticipate that accurate accounts of anatomy in these taxa, particularly with respect to arrangement of the dorsal components of the skeleton, will be more challenging. Third, some aspects of the study of fossil gill skeletons via computed tomography is limited by resolution and contrast available in tomograms. Although the resolution of scans used in this study range from 0.032-0.107 mm, small structures like posterior upper pharyngeal toothplates lack the kind of detail available in modern comparative material. This is exacerbated to some degree by density contrast between

947 fossil bone and surrounding rock, which varies from deposit to deposit, and sometimes
948 even within deposits. However, these issues represent technical limitations that we
949 anticipate will be ameliorated to some degree in the future, rather than fundamental
950 challenges inherent to fossil material itself.
951 Despite the limitations mentioned above, computed tomography represents an attractive
952 alternative to traditional destructive or acid-preparation techniques, largely due to the
953 retention of vital positional information. Furthermore, specimens subjected to historical
954 acid preparation are frequently fragile, fragmentary and difficult to interpret, typically at
955 the expense of character information. In sum, while there are clearly obstacles that
956 prevent the study of gill-arch skeletons in the level of detail available for modern
957 specimens, it is nevertheless clear that the subset of data available in paleontological
958 material via tomography still can make useful contributions to the placement of fossil
959 taxa.
960
961 **Conclusions**
962 The three-dimensionally preserved skulls of seven genera of Cretaceous-Paleogene
963 aulopiforms were examined using μCT in order to extract anatomical details of the branchial
964 skeleton. The completeness and degree of articulation of the gill skeletons reconstructed from
965 these fossils varies from near-intact (†*Argillichthys*) to highly fragmentary (†*Cimolichthys*),
966 with clear consequences for the number of cladistic characters that can be evaluated (27 of 33
967 for †*Argillichthys*, 5 of 33 for †*Cimolichthys*). While it is possible to assess features
968 pertaining to the structure of individual branchial bones in most specimens, characters
969 requiring positional information could only be evaluated in specimens showing minimal
970 disruption, and could not be obtained at all from acid prepared specimens. All taxa examined
971 show the presence of the key aulopiform gill-arch synapomorphy (presence of a long

uncinate process of the second epibranchial) apart from †*Halec eupterygius* and †*Cimolichthys lewesiensis*, where a lack of mineralization or damage to the gill skeleton prevents assessment of state. We inferred the position of fossils within aulopiform phylogeny using a cladistic analysis based on the set of branchial characters presented by (Davis 2010) and with relationships among living species constrained to match the 'total evidence' topology presented by that study. We corroborate past associations between †*Apateodus corneti,* †*Cimolichthys lewesiensis* and †*Halec eupterygius* with alepisauroids, although they are not grouped with the same modern lineages and some have an uncertain placement within this clade. †*Argillichthys toombsi* and †*Labrophagus esocinus* are resolved as stem synodontids, while †*Aulopopsis depressifrons* is considered Aulopiformes *incertae sedis.* †'*Sardinioides*' *illustrans* is shown to be an aulopiform, and thus not closely related to the type species of the genus †*Sardinioides*, which is a myctophiform. Our constrained analysis places †'*S.*' *illustrans* as a stem aulopid or stem paralopid. This work establishes the utility of μCT as a tool for accessing ossified features of gill-arch anatomy in three-dimensionally preserved fossil teleost skulls, opening up a largely untapped source of characters for establishing the relationships of extinct taxa to living species. While three-dimensionally preserved skulls are rarer than compression fossils, they are known from numerous horizons associated with important intervals in teleost evolution (Friedman et al. 2015). Targeted study of this material, particularly that attributed to modern groups with well-defined synapomorphies relating to the gill skeleton, has the potential to more definitively constrain the position of fossil species whose placements are based on argumentation from overall similarity.

Supplementary Material

Mimics (.mcs) files, DICOM Stacks and PLY files are available for all taxa figured in this

997 study at:

998

999 **Acknowledgements**

1000 The authors thank Farah Ahmed, Emma Bernard, Zerina Johanson, Rebecca
1001 Summerfield, and Dan Sykes for access to the collections and assistance with scanning at
1002 the Natural History Museum, London. Matt Riley at the Sedgwick Museum, University
1003 of Cambridge, and R. van Zelst at the Naturalis Biodiversity Centre, who facilitated the
1004 loan of specimens for scanning and study. Matt Davis, St. Cloud State University
1005 provided the character list, data matrix and sequence alignment that forms the basis of
1006 this study. We also thank David Johnson, Smithsonian National Museum of Natural
1007 History, for comments on an earlier draft of this study, and constructive conversation
1008 on the anatomy of teleost gill skeletons, more generally. Paul Shepherd, British
1009 Geological Survey provided access to specimens and Simon Harris, British Geologial
1010 Survey, provided photos of †*Apateodus striatus*. We also thank the reviewers, Mike
1011 Newbrey and Valéria Gallo, for their thorough and constructive feedback on this
1012 manuscript. This research was supported by a NERC studentship to HB on the DTP
1013 Environmental Research (NE/L0021612/1), a Leverhulme Project Grant (RPG-2012-658)
1014 and Leverhulme Prize (PLP-2012-130), both to MF, and a Junior Research Fellowship from
1015 Christ Church, Oxford, to SG.

1016

1017 **REFERENCES**

1018 **Agassiz, L.** 1833-44. *Recherches sur les poisons fossils,* 5 vols., 1420 pp., 396 pls., with
1019 supplement. Neuchatel, Petitpierre.

1020 **Baldwin, C. C. & Johnson, G. D.** 1996. Interrelationships of Aulopiformes. Pp 355–404
1021 in M.L.J. Stiassny, L.R. Parenti & G. D. Johnson (eds) *Interrelationships of Fishes*.

1022 Academic Press, San Diego.
1023 **Beckett, H. T. & Friedman, M.** 2016. The one that got away from Smith Woodward:
1024 cranial anatomy of *Micrornatus* (Acanthomorpha: Scombridae) revealed using
1025 computed microtomography. Pp 337–353 in Z. Johanson, P. M. Barrett, M. Richter &
1026 M. Smith (eds) *Arthur Smith Woodward: His Life and Influence on Modern*
1027 *Vertebrate Palaeontology.* Geological Society Special Publication 430, London.
1028 **Betancur-r, R., Broughton, R. E., Wiley, E. O., Carpenter, K., López, J. A., Li, C.,**
1029 **Holcroft, N. L., Arcila, D., Sanciangco, M., Cureton II, J. C., Zhang, F., Buser, T.,**
1030 **Campbell, M. A., Ballesteros, J. A., Roavaron, A., Willis, S., Borden, W. C.,**
1031 **Rowley, T., Reneau, P. C., Hough, D. J., Lu, G., Grande, T., Arratia, G. & Orti,**
1032 **G.** 2013. The Tree of Life and a New Classification of Bony Fishes. *PLOS Currents*
1033 *Tree of Life*, (0732988).
1034 **Carvalho, M., Bockmann, F. A. & de Carvalho, M. R.**. 2013. Homology of the fifth
1035 epibranchial and accessory elements of the ceratobranchials among Gnathostomes:
1036 insights from the development of ostariophysans. *PLOS ONE 8(4):e62389.*
1037 **Casier, E.** 1966. *Faune icthyologique du London Clay*. British Museum (Natural
1038 History), London.
1039 **Chen, W. J., Santini, F., Carnevale, G., Chen, J. N., Liu, S. H., Lavoué, S. & Mayden, R.**
1040 **L.** 2014. New insights on early evolution of spiny-rayed fishes (Teleostei:
1041 Acanthomorpha). *Frontiers in Marine Science*, **1**, 1–53.
1042 **Choo, B., Long, J. A. & Trinajstic, K.** 2009. A new genus and species of basal
1043 actinopterygian fish from the Upper Devonian Gogo Formation of Western Australia. *Acta*
1044 *Zoologica*, **90**(s1), 194–210.
1045 **Davis, M. P.** 2010. Evolutionary relationships of the Aulopiformes (Euteleostei: Cy-
1046 closquamata: a molecular and total evidence approach. Pp 431–470 in J. S. Nelson, H.

P. Schultze, & M. V. H. Wilson (eds) *Origin and Phylogenetic Interrelationships of Teleosts,* Verlag Dr. Friedrich Pfeil, München.

Davis, M. P. & Fielitz, C. 2010. Estimating divergence times of lizardfishes and their allies (Euteleostei: Aulopiformes) and the timing of deep-sea adaptations. *Molecular Phylogenetics and Evolution*, **57**(3), 1194–208.

Dietze, K. 2009. Morphology and phylogenetic relationships of certain neoteleostean fishes from the Upper Cretaceous of Sendenhorst, Germany. *Cretaceous Research*, **30**(3), 559–574.

Dixon, F. 1850. The Geology and Fossils of the Tertiary and Cretaceous Formations of Sussex. Longman, Brown, Green and Longmans, London, 422 pp

Fielitz, C. 2004. The phylogenetic relationships of the †Enchodontidae (Teleostei: Aulopiformes). Pp 619–634 in G. Arratia, M. V. H. Wilson & R. Cloutier (eds) *Recent Advances in the Origin and Early Radiation of Vertebrates*. Verlag Dr. Friedrich Pfeil, München.

Fielitz, C. & Gonzáles Rodríguez, K. 2008. A new species of *Ichthyotringa* from the El Doctor Formation (Cretaceous), Hidalgo, Mexico. Pp 373–388 in G. Arratia, H.-P. Schultze, & M. V. H. Wilson (eds) *Mesozoic Fishes 4 – Homology and Phylogeny*, Verlag Dr. Friedrich Pfeil, München.

Fielitz, C. & González-Rodríguez, K. 2010. A new species of enchodus (Aulopiformes: Enchodontidae) from the Cretaceous (Albian to Cenomanian) of Zimapán, Hidalgo, México. *Journal of Vertebrate Paleontology* **30**(5), 1343–1351.

Fink, W. L. & Weitzman, S. H. 1982. Relationships of the stomiiform fishes (Teleostei), with a description of *Diplophos*. Bulletin of the Museum of Comparative Zoology **150**, 31–93.

Forey, P. L., Yi, L., Patterson, C. & Davies, C. E. 2003. Fossil fishes from the Cenomanian

(Upper Cretaceous) of Namoura, Lebanon. *Journal of Systematic Palaeontology*, **1**(4), 227–330.

Forir, H. 1887. *Contributions à l'étude du système crétacé de la Belgique* Liège: Imprimerie H. Vaillant-Carmanne 34pp.

Friedman, M. 2012. Ray-finned fishes (Osteichthyes, Actinopterygii) from the type Maastrichtian, the Netherlands and Belgium. Pp. 113-142 in J.W.M. Jagt, S.K. Donovan & E.A. Jagt-Yazykova (eds) *Fossils of the Type Maastrichtian (Part 1)*. Scripta Geologica Special Issue 8.

Friedman, M., Beckett, H.T., Close, R.A. & Johanson, Z. 2016. The English chalk and London Clay: two remarkable British bony fish Lagerstätten. Pp 165–200 in Z. Johanson, P. M. Barrett, M. Richter & M. Smith (eds) *Arthur Smith Woodward: His Life and Influence on Modern Vertebrate Palaeontology.* Geological Society Special Publication 430, London.

Gallo, V. & Coelho, P.M. 2008. First occurrence of an aulopiform fish in the Barremian of the Sergipe-Alagoas Basin, northeastern Brazil. Pp 351–371 in G. Arratia, H.-P. Schultze, & M. V. H. Wilson (eds) *Mesozoic Fishes 4 – Homology and Phylogeny*, Verlag Dr. Friedrich Pfeil, München.

Gardiner, B. G. 1984. Devonian palaeoniscid Fishes: new Specimens of *Mimia* and *Moythomasia* from the Upper Devonian of Western Australia. *Bulletin of the British Museum of Natural History (Geology)*, **37**, 173–428.

Giles, S., Darras, L., Clement, G., Blieck, A. & Friedman, M. 2015. An exceptionally preserved Late Devonian actinopterygian provides a new model for primitive cranial anatomy in ray-finned fishes. *Proceedings of the Royal Society B,* **282** (20151485), 1–10.

Gill, T. N. 1862. *Catalogue of the fishes of the eastern coast of North America, from Greenland to Georgia.* Proceedings of the Academy of Natural Sciences of Philadelphia,

pp 1–63.

Goody, P.C. 1969. The relationships of certain Upper Cretaceous teleosts with special reference to the myctophoids. *Bulletin of the British Museum (Natural History): Geology, Supplement*, **7**, 1–255.

Grande, L. & Bemis, W.E. 1998. A comprehensive phylogenetic study of amiid fishes (Amiidae) based on comparative skeletal anatomy. An empirical search for interconnected patterns of natural history. *Journal of Vertebrate Paleontology*, **18**(S1), pp.1–696.

Jagt, J.W.M. & Jagt-Yazykova, E.A. 2012. Stratigraphy of the type Maastrichtian – a synthesis. Pp 5–32 in Jagt, J.W.M. & Jagt-Yazykova, E.A. (eds) Fossils of the type Maastrichtian (Part 1), *Scripta Geologica Special Issue,* **8**.

Jarvik, E. 1980. *Basic structure and evolution of vertebrates,* Vol. 1. Academic Press, London.

Johnson, R. K. 1982. Fishes of the families Evermanellidae and Scopelarchidae: systematics, morphology, interrelationships, and zoogeography. *Fieldiana (Zoology), New Series*, **12**, 1–252.

Johnson, G.D. 1992. Monophyly of the euteleostean clades: Neoteleostei, Eurypterygii, and Ctenosquamata. *Copeia*, 8–25.

Johnson, G. D., Baldwin, C. C., Okiyama, M. & Tominaga, Y. 1996. Osteology and relationships of *Pseudotrichonotus altivelis* (Teleostei: Aulopiformes: Pseudotrichonotidae). *Ichthyological Research*, **43**(1), 17–45.

Jordan, D. S. 1905. A Guide to the Study of Fishes. H. Holt and Co., New York: xxii + 589 pp.

Khalloufi, B., Ouarhache, D. & Lelièvre, H. 2010. New paleontological and geological data about Jebel Tselfat (Late Cretaceous of Morocco). *Historical Biology*, **22**, 57–70.

Kruizinga, P. 1924. *†Apateodus corneti* (For.) in the Senonian beds of the southern part

of Limburg (Netherlands). *Proceedings of the Science Section of the Koninklijke Nederlandse Akademie van Wetenschappen,* **27**, 293–312.

Leidy, J. 1857. *Notices of some remains of extinct fishes*. Proceedings of the Academy of Natural Sciences of Philadelphia, **9**, 167–168.

McAllister, D. E. 1968. The evolution of branchiostegals and associated opercular, gular and hyoid bones and the classification of teleostome fishes, living and fossil. *Bulletin of the National Museum of Canada,* **221**, 1–239.

Miles, R. S. 1973. *Articulated Acanthodian Fishes from the Old Red Sandstone of England: With a Review of the Structure and Evolution of the Acanthodian Shoulder-girdle*. British Museum (Natural History), London, 102 pp, 21 pls.

Müller, J. 1845. Über den Bau und die Grenzen der Ganoiden, und über das natürliche System der Fische. Arch Naturgesch, **11**, 91–141.

Near, T. J., Eytan, R. I., Dornburg, A., Kuhn, K. L., Moore, J. A., Davis, M. P., Wainwright, P. C., Friedman, M. & Smith, W.L. 2012. Resolution of ray-finned fish phylogeny and timing of diversification. *Proceedings of the National Academy of Sciences*, **109**(34), 13698–13703.

Near, T. J., Dornburg, A., Eytan, R. I., Keck, B. P., Smith, W. L., Kuhn, K. L., Moore, J. A., Price, S. A., Burbrink, F. T., Friedman, M. & Wainwright, P. C. 2013. Phylogeny and tempo of diversification in the superradiation of spiny-rayed fishes. *Proceedings of the National Academy of Sciences*, **110**(31), 12738–12743.

Nelson, G. J. 1969. Gill arches and the phylogeny of fishes, with notes on the classification of vertebrates. *Bulletin of the American Museum of Natural History*, **141**, 474–552.

Nelson, J. S. 2006. *Fishes of the World.* John Wiley Son, Inc., Hoboken, New Jersey, 624 pp.

Nelson, J. S., Grande, T. & Wilson, M. V. H. 2016. *Fishes of the world*. Fifth edition, John

1147 Wiley and Sons, New Jersey, 707pp.
1148 **Newbrey, M.G. & Konishi, T.** 2015. A new lizardfish (Teleostei, Aulopiformes) from
1149 the Late Cretaceous Bearpaw Formation of Alberta, Canada, with a revised diagnosis
1150 of †*Apateodus* (Aulopiformes, Ichthyotringoidei). *Journal of Vertebrate Paleontology,*
1151 **35**(3), e918042.
1152 **Nielsen, E.** 1942. Studies on Triassic fishes from East Greenland. I – *Glaucolepus* and
1153 *Boreosomus Meddeleser øm Gronland,* **138**, 1–403.
1154 **O'Leary, M. & Geisler, J.** 1999. The position of Cetacea within Mammalia: Phylogenetic
1155 analysis of morphological data from extinct and extant taxa. *Systematic Biology* **48**, 455–
1156 490.
1157 **Patterson, C.** 1964. A review of Mesozoic acanthopterygian fishes, with special reference to
1158 those of the English Chalk. *Philosophical Transactions of the Royal Society of London.*
1159 *Series B, Biological Sciences*, **247**, 213–482.
1160 **Patterson, C. & Johnson, G. D.** 1995. The intermuscular bones and ligaments of teleostean
1161 fishes. *Smithsonian contributions to zoology (USA)* **559**, 1–87.
1162 **Patterson, C. & Rosen, D. E.** 1977. Review of ichthyodectiform and other Mesozoic teleost
1163 fishes and the theory and practice of classifying fossils. *Bulletin of the American Museum*
1164 *of Natural History*, **158**, 81–172.
1165 **Pradel, A., Maisey, J., Tafforeau, P., Mapes, R. & Mallatt, J.** 2014. A Palaeozoic shark
1166 with osteichthyan-like branchial arches. *Nature* **509**, 7502, 608–611
1167 **Rosen, D. E.** 1973. Interrelationships of higher euteleostean fishes. *In*: Greenwood, P.H.,
1168 Miles, R.S., and Patterson, C. (eds) *Interrelationships of Fishes*, 297–513. Academic
1169 Press, London.
1170 **Sato, T. & Nakabo, T.** 2002. Paraulopidae and *Paraulopus*, a new family and genus of
1171 aulopiform fishes with revised relationships within the order. *Ichthyological Research*,

49(1973), 25–46.

Silva, H. M. A. 2011 *Biogeografia e sistemática dos peixes Aulopiformes* (PhD. Thesis), Universidade do Estado do Rio de Janeiro, Instituto de Biologia Roberto Alcântara Gomes, Programa de Pós-graduação em Ecologia e Evolução. 256 pp.

Silva, H. M. A. & Gallo, V. 2011. Taxonomic review and phylogenetic analysis of Enchodontoidei (Teleostei: Aulopiformes) *Anais da Academia Brasileira de Ciências,* **83**(2), 483–511.

Stensiö, E. A. 1969. Elasmobranchiomorphi Placodermata Arthrodires. *Traité de paléontologie*, **4**(2), 71–692.

Stiassny, M. L. J., Parenti, L. R. & Johnson, G. D. 1996. Basal Ctenosquamate relationships and the interrelationships of the myctophiform (Scopelomorph) fishes. Pp 405–426 in M.L.J. Stiassny, L.R. Parenti and G. D. Johnson (eds) *Interrelationships of Fishes*. Academic Press, San Diego.

Swofford, D. L. 2002**.** PAUP*. Phylogenetic Analysis Using Parsimony (*and Other Methods). Version 4.0a152. Sinauer Associates, Sunderland, Massachusetts.

Taverne, L. 2006. Révision d'*Ichthyotringa africana*, poisson marin (Teleostei, Aulopiformes) du Crétacé supérieur de la Mésogée eurafricaine. Considérations sur les relations phylogénétiques du genre *Ichthyotringa*. *Belgium Journal of Zoology,* **136**, 31–41.

von der Marck, W. 1858**.** Uebereinige Wirbelthiere, Krusterund Cephalopoden der Westphälischen Kreide. *Zeitschrift der Deutschen Geologischen Gesellschaft, Berlin* **10**, 231–271, 2 pls.

Woodward, A. S. 1901. *Catalogue of Fossil Fishes in the British Museum (Natural History). Part IV. Containing the Actinopterygian Teleostomi of the Suborders Isospondyli (in Part), Ostariophysi, Apodes, Percesoces, Hemibranchii, Acanthopterygii, and*

Anacanthini. Trustees of the British Museum (Natural History), London.

Woodward, A. S. 1902-1912. *The fossil fishes of the English Chalk.* Monograph of the Palaeontographical Society, London, viii+264 pp., 54 pls.

Wiley, E. O. & Johnson, G. D. 2010. A teleost classification based on monophyletic groups. Pp 123–182 in J. S. Nelson, H. P. Schultze, and M. V. H. Wilson (eds) *Origin and Phylogenetic Interrelationships of Teleosts,* Verlag Dr. Friedrich Pfeil, München.

1205 Fig. 1. Photographs of (**A**) †*Argillichthys toombsi* (NHMUK PV P42519), (**B**)
1206 †*Labrophagus esocinus* (CAMSM TN 4286), (**C**) †*Apateodus corneti* (RGM 446950),
1207 (**D**) †*Cimolicthys lewesiensis* (NHMUK PV P5491), (**E**) †*Halec eupterygius* (NHMUK
1208 PV P5662), (**F**) †*Aulopopsis depressifrons* (NHMUK PV P26712), and (**G**) †*Sardinioides*
1209 *illustrans* (NHMUK PV P3977). Scale bars: 10 mm.
1210
1211 Fig. 2. Gill skeleton of †*Argillichthys toombsi* (NHMUK PV P42519) in dorsal view.
1212 Renderings of **(A)** complete gill skeleton (ventral arches: pale green; dorsal arches: mid-
1213 green; urohyal: dark green), (**B**) ventral gill skeleton only, and **(C**) dorsal gill skeleton
1214 only. Interpretive drawings of **(D**) ventral gill skeleton, and (**E**) dorsal gill skeleton. Scale
1215 bar 10 mm. BB - basibranchial, BHTP - basihyal toothplate, CB - ceratobranchial, EB -
1216 epibranchial, HB - hypobranchial, PB - pharyngobranchial, U - urohyal; UP, uncinate
1217 process; UPT - upper pharyngeal toothplate.
1218
1219 Fig. 3. Gill skeleton of †*Labrophagus esocinus* (CAMSM TN 4286) in dorsal view.
1220 Renderings of (**A**) complete gill skeleton (ventral arches: pale green; dorsal arches: mid-
1221 green; urohyal: dark green) in dorsal view, (**B**) ventral gill skeleton only in dorsal view,
1222 (**C**) dorsal gill skeleton in dorso-lateral view and (**D**) dorsal gill skeleton in dorsal view**.**
1223 Interpretive drawings of (**E**) ventral gill skeleton in dorsal view, (**F**) dorsal gill skeleton
1224 in dorso-lateral view and (**G**) dorsal gill skeleton in dorsal view. Scale bar 10 mm. BB -
1225 basibranchial, BHTP - basihyal tooth plate, CB - ceratobranchial, EB - epibranchial, HB
1226 - hypobranchial, PB - pharyngobranchial, U - urohyal, UP - uncinate process.
1227
1228 Fig. 4. Gill skeleton of †*Apateodus corneti* (RGM 446950). Renderings in dorsal view of
1229 **(A**) complete gill skeleton (ventral arches: pale green; dorsal arches: mid-green), (**B**)

ventral gill skeleton only, and **(D)** dorsal gill skeleton only. Interpretive drawings of **(C)** ventral gill skeleton, and (**E**) dorsal gill skeleton. (**F**) Rendering of epibranchial 2 in ventral view (**G**) interpretive drawing of epibranchial 2 in ventral view. Scale bar 10 mm. BB - basibranchial, BBTP - basibranchial toothplate, CB - ceratobranchial, EB - epibranchial, HB - hypobranchial, PB - pharyngobranchial, UP - uncinate process.

Fig. 5. Gill skeleton elements of †*Apateodus striatus* (BGS GSM 26241). (**A**) Urohyal in dorsal view, (**B**) basihyal toothplate in ventral (left) and dorsal (right) view, (**C**) hypobranchial in ventral view, (**D**) ceratobranchials in dorsal view, (**E**) ceratobranchial 5 in dorsal view, (**F**) epibranchials in ventral view, with possible rod-like ceratobranchials attached by consolidant, (**G**) left epibranchial 3 and upper pharyngeal tootplate 4. CB - ceratobranchial, EB - epibranchial, UP - uncinate process, UPT - upper pharyngeal toothplate. Photo credit: Simon Harris, British Geological Survey © NERC.

Fig. 6. Gill skeleton of †Cimolicthys lewesiensis in dorsal view. (**A**) render of complete gill skeleton of NHMUK PV P5491, (**B**) interpretive drawing of complete gill skeleton of NHMUK PV P5491, (**C**) photograph of the urohyal of NHMUK PV P1810a and (**D**) photograph of fragments of ceratobranchial 5 of NHMUK PV P1810a.. Scale bar 10 mm. BB - basibranchial, BHTP - basihyal toothplate, HB - hypobranchial, CB - ceratobranchial.

Fig. 7. Gill skeleton of †*Halec eupterygius* (NHMUK PV P5662). Renderings in dorsal view of (**A**) complete gill skeleton (ventral arches: pale green; dorsal arches: mid-green; urohyal: dark green) and (**B**) ventral gill skeleton and urohyal. (**C**) Interpretive drawing of ventral gill skeleton and urohyal. (**D**) Rendering in dorsal view of dorsal gill skeleton

only. (**E**) Interpretive drawing of dorsal gill skeleton. Renderings in lateral view of (**F**) complete gill skeleton (ventral arches: pale green; dorsal arches: mid-green; urohyal: dark green), (**G**) ventral gill skeleton and urohyal, and (**H**) dorsal gill skeleton only. Interpretive drawings of (**I**) dorsal gill skeleton and urohyal, and (**J**) ventral gill skeleton. (**K**) Photograph of the gill skeleton of NHMUK PV OR 43392 and (**L**) drawing of the gill skeleton of NHMUK PV OR 43392. Scale bars 10 mm. aC - anterior ceratohyal, BB - basibranchial, CB - ceratobranchial, EB - epibranchial, HB - hypobranchial, PB - pharyngobranchial, pC - posterior ceratohyal, U - urohyal.

Fig. 8. Gill skeleton of †*Aulopopsis depressifrons* (NHMUK PV P26712) in dorsal view. Renderings of (**A**) complete gill skeleton (ventral arches: pale green; dorsal arches: mid-green), (**B**) ventral gill skeleton only, (**C**) dorsal gill skeleton only. Interpretive drawings of (**D**) ventral gill skeleton, and (**E**) dorsal gill skeleton. Scale bar 10 mm. BB - basibranchial, BHTP - basihyal toothplate, CB - ceratobranchial, EB - epibranchial, HB - hypobranchial, PB - pharyngobranchial, U - urohyal.

Fig. 9. Gill skeleton of †*Sardinioides illustrans* (NHMUK PV P3977) in dorsal view. Renderings of (**A**) complete gill skeleton (ventral arches: pale green; dorsal arches: mid-green; urohyal: dark green), (**B**) ventral gill skeleton and (**C**) dorsal gill skeleton. Interpretive drawings of (**D**) ventral gill skeleton, and (**E**) drawing of dorsal gill skeleton. Scale bar 10 mm. BB - basibranchial, BHTP - basihyal tooth plate, CB - ceratobranchial, EB - epibranchial, HB - hypobranchial, PB - pharyngobranchial, U - urohyal, UP - uncinate process, UPT - upper pharyngeal toothplate.

Fig. 10. Distribution of gill skeleton characters in Aulopiformes, based on the Bayesian

1280 'total evidence' topology presented by Davis (2010: fig. 7). Some clades collapsed to
1281 family level. Apomorphies mapped based on parsimony reconstructions that are
1282 consistent between ACCTRAN and DELTRAN optimizations. Grey branches in tree
1283 indicate weak statistical support in either the Bayesian or parsimony reconstructions
1284 (after Davis 2010: fig. 8), for node support see Davis 2010: fig. 7). For a list of
1285 characters and states, along with character numbers as they appear in Davis (2010), see
1286 Supplementary Information. Images redrawn from Nelson (2006).
1287
1288 Fig. 11. Reconstructions of the gill skeletons of (**A**) †*Argillichthys toombsi* (NHMUK
1289 PV P42519), (**B**) †*Labrophagus esocinus* (CAMSM TN 4286), (**C**) †*Apateodus corneti*
1290 (RGM 446950), (**D**) †*Cimolicthys lewesiensis* (NHMUK PV P5491), (**E**) †*Halec*
1291 *eupterygius* (NHMUK PV P5662), (**F**) †*Aulopopsis depressifrons* (NHMUK PV P26712),
1292 and (**G**) †*Sardinioides illustrans* (NHMUK PV P3977). Components not preserved or
1293 unclear in specimens are hypothetical and are shaded grey. Not to scale.
1294
1295 Fig. 12. Placements of fossil taxa within Aulopiformes based upon a constrained
1296 cladistics analysis using gill-arch characters. Highlighted branches indicate the multiple
1297 possible placements for †*Halec eupterygius* (red branches) and †*Sardinioides illustrans*
1298 (blue branches). Non-aulopiform outgroups were included in the analysis (see Methods)
1299 but have been pruned from this figure for clarity.
1300

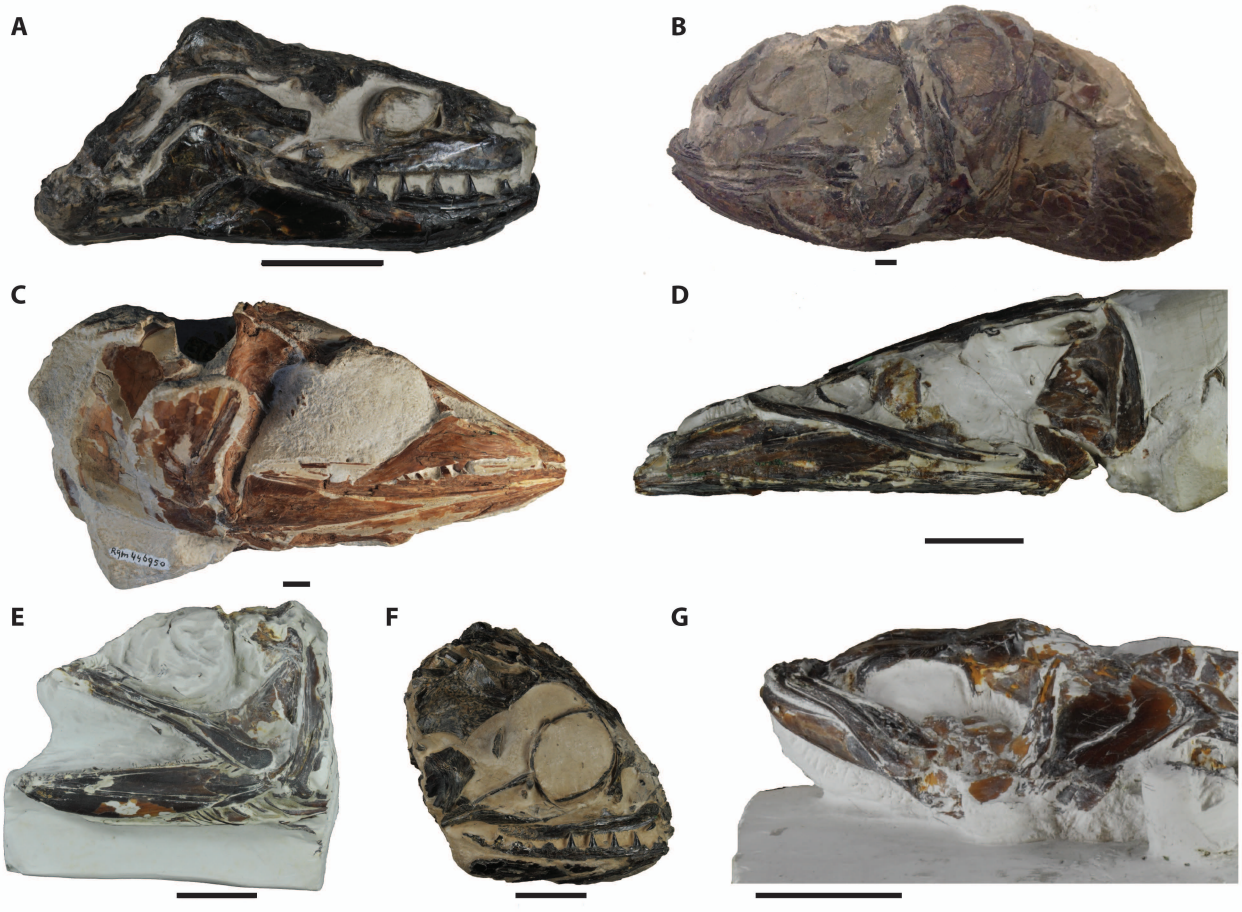
A
B
C
D
E
F
G

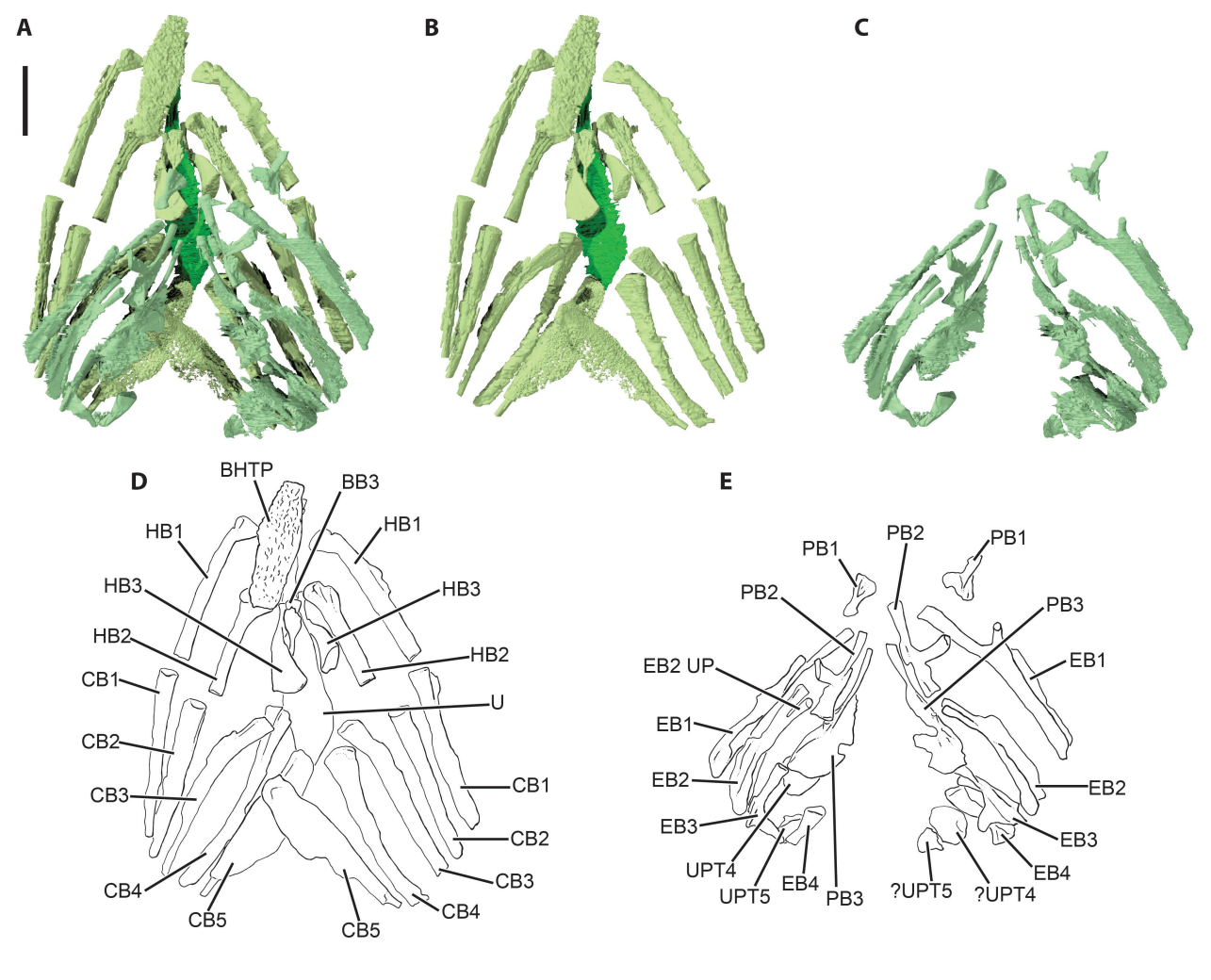
A
B
C
D
BHTP
BB3
HB1
HB1
HB3
HB3
HB2
HB2
CB1
U
CB2
CB3
CB1
CB2
CB3
CB4
CB5
CB4
CB5
E
PB1
PB2
PB1
PB2
PB3
EB2 UP
EB1
EB1
EB2
EB2
EB3
EB3
UPT4
UPT5
EB4
PB3
?UPT5
?UPT4
EB4

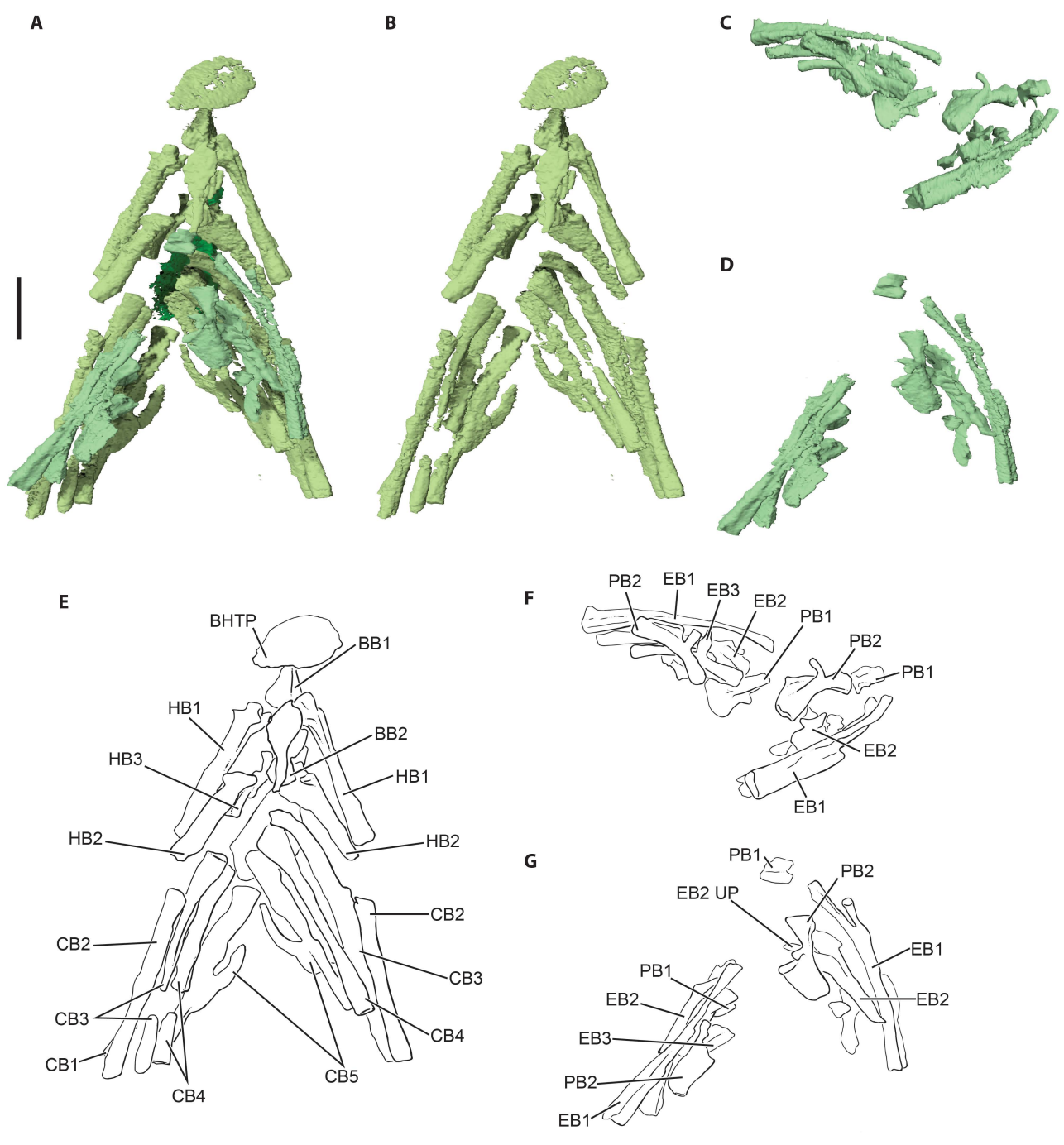
A
B
C
D
E
BHTP
BB1
HB1
BB2
HB3
HB1
HB2
HB2
CB2
CB2
CB3
CB3
CB4
CB1
CB5
CB4
F
PB2
EB1
EB3
EB2
PB1
PB2
PB1
EB2
EB1
G
PB1
PB2
EB2 UP
EB1
PB1
EB2
EB2
EB3
PB2
EB1

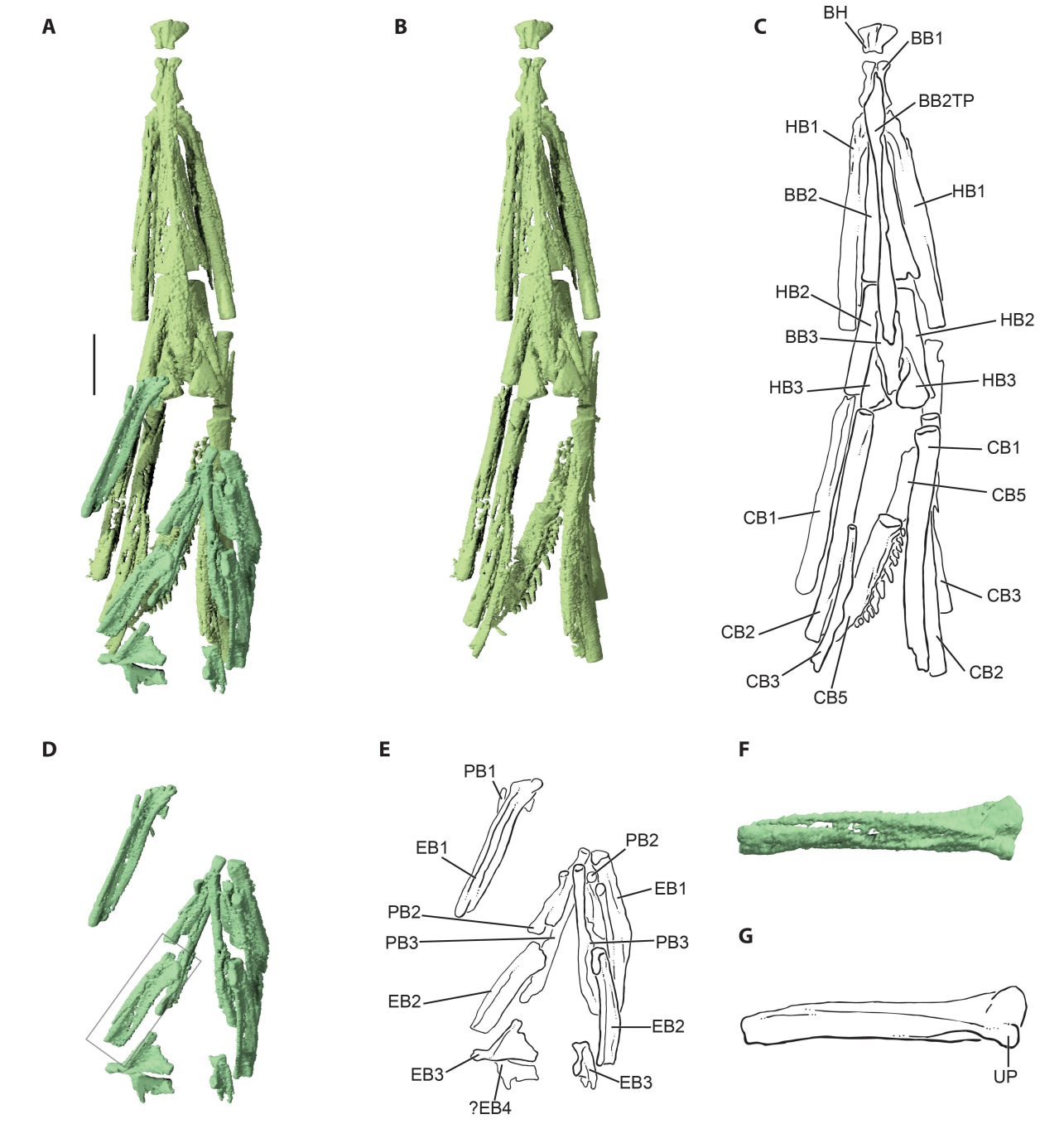
A
B
C
BH
BB1
BB2TP
HB1
BB2
HB1
HB2
HB2
BB3
HB3
HB3
CB1
CB5
CB1
CB3
CB2
CB3
CB5
CB2
D
E
PB1
EB1
PB2
EB1
PB2
PB3
PB3
EB2
EB2
EB3
EB3
?EB4
F
G
UP

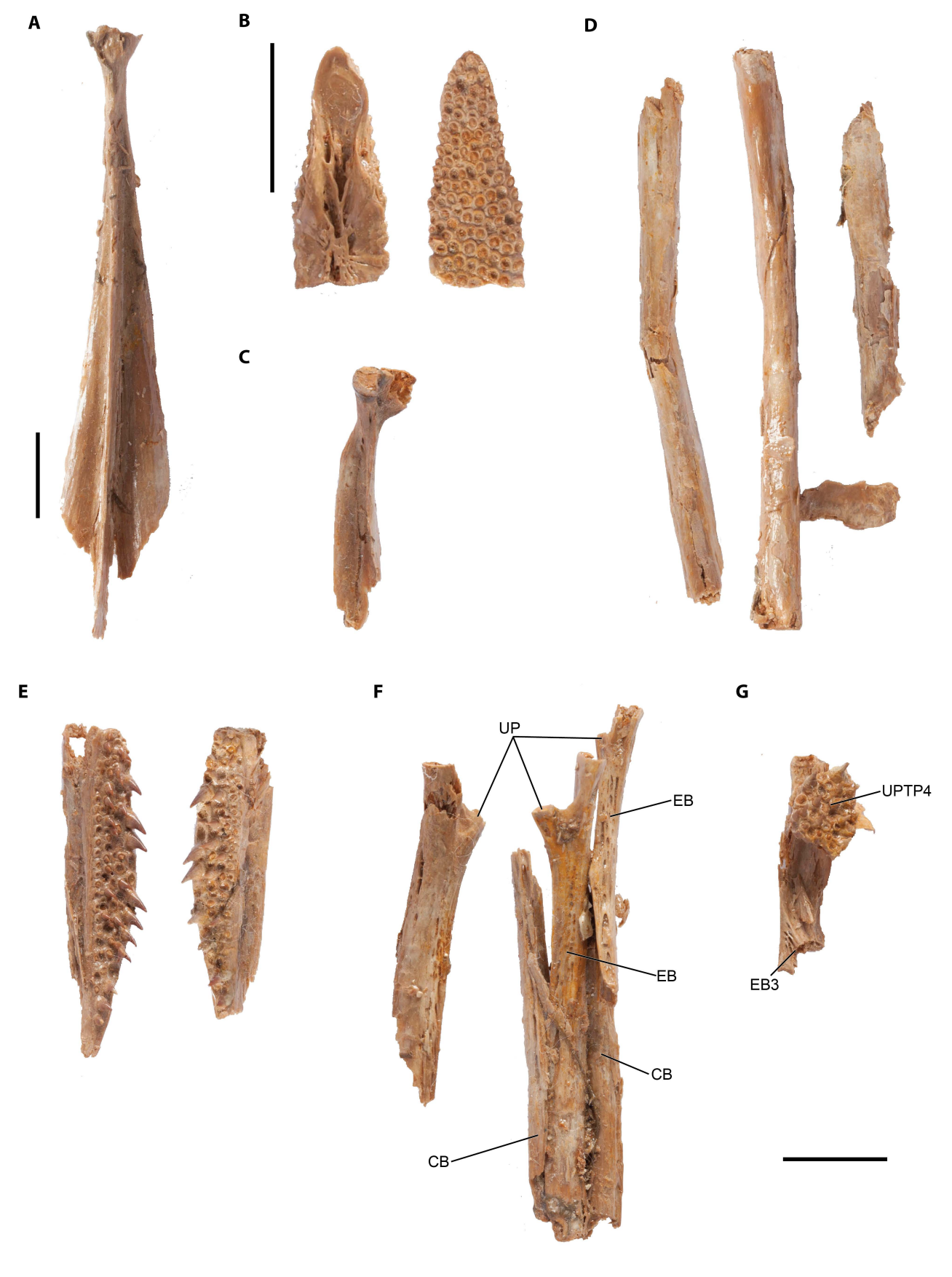
A
B
C
D
E
F
G
UP
EB
EB
CB
CB
UPTP4
EB3

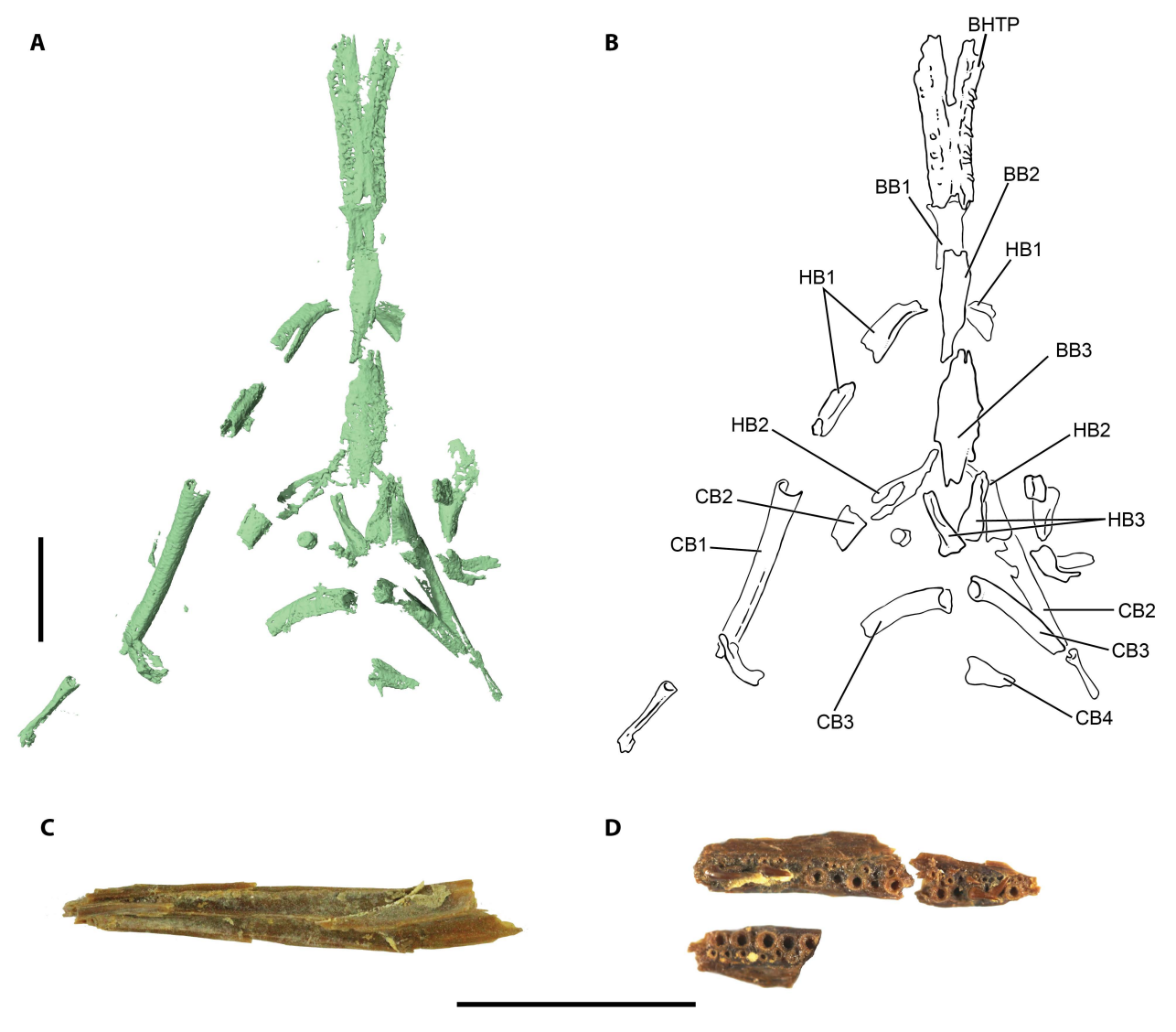
A
B
BHTP
BB1
BB2
HB1
HB1
BB3
HB2
HB2
CB2
HB3
CB1
CB2
CB3
CB3
CB4
C
D

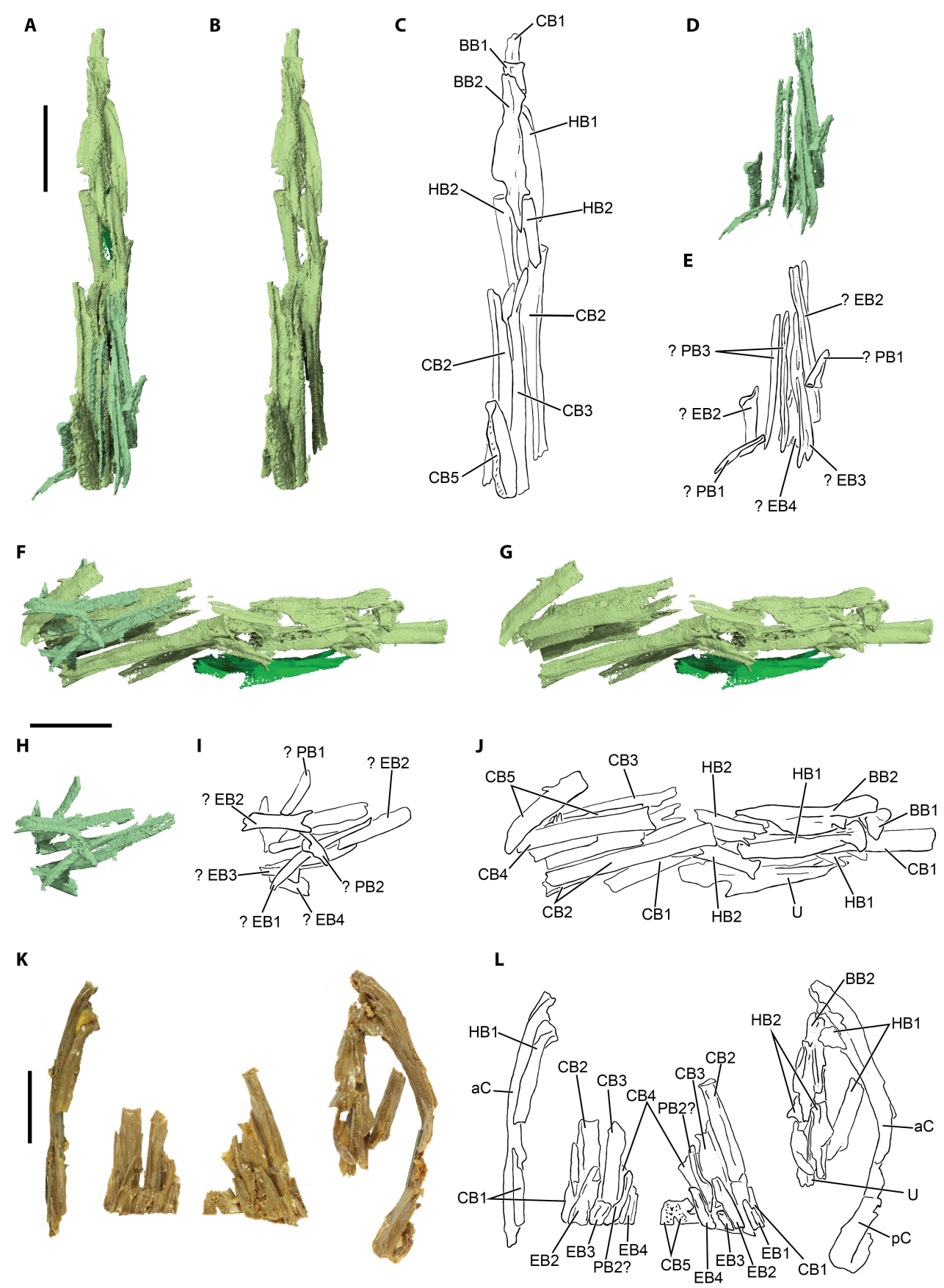
A
B
C
CB1
BB1
BB2
HB1
HB2
HB2
CB2
CB2
CB3
CB5
D
E
? EB2
? PB3
? PB1
? EB2
? PB1
? EB3
? EB4
F
G
H
I
? PB1
? EB2
? EB2
? EB3
? PB2
? EB1
? EB4
J
CB5
CB3
HB2
HB1
BB2
BB1
CB1
CB4
CB2
CB1
HB2
U
HB1
K
L
HB1
aC
CB2
CB3
CB4
PB2?
CB2
CB3
BB2
HB2
HB1
aC
U
pC
CB1
EB2
EB3
PB2?
EB4
CB5
EB4
EB3
EB2
EB1
CB1

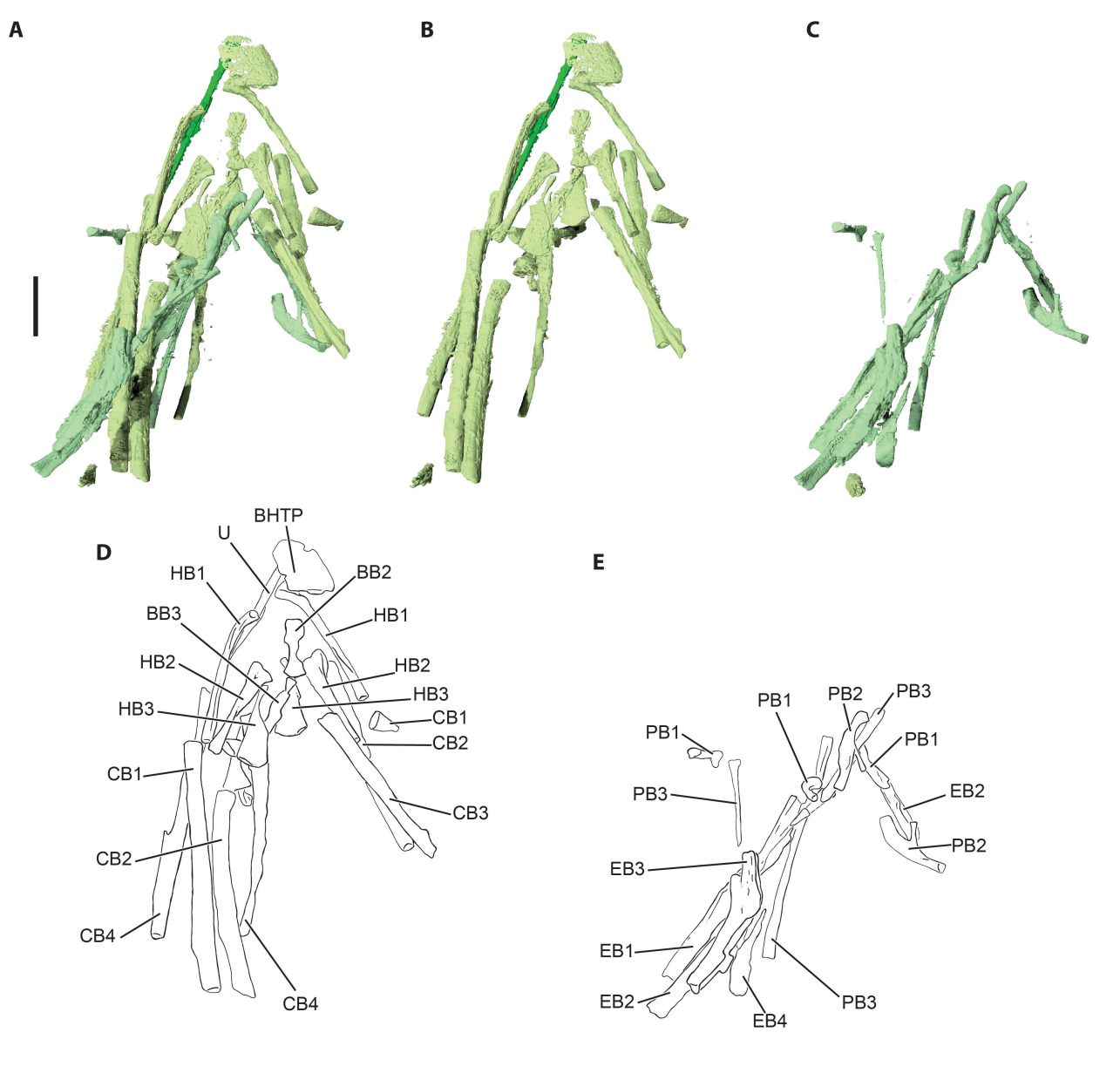
A
B
C
D
BHTP
U
HB1
BB2
BB3
HB1
HB2
HB2
HB3
HB3
CB1
CB2
CB1
CB3
CB2
CB4
CB4
E
PB1
PB2
PB3
PB1
PB1
PB3
EB2
PB2
EB3
EB1
EB2
PB3
EB4

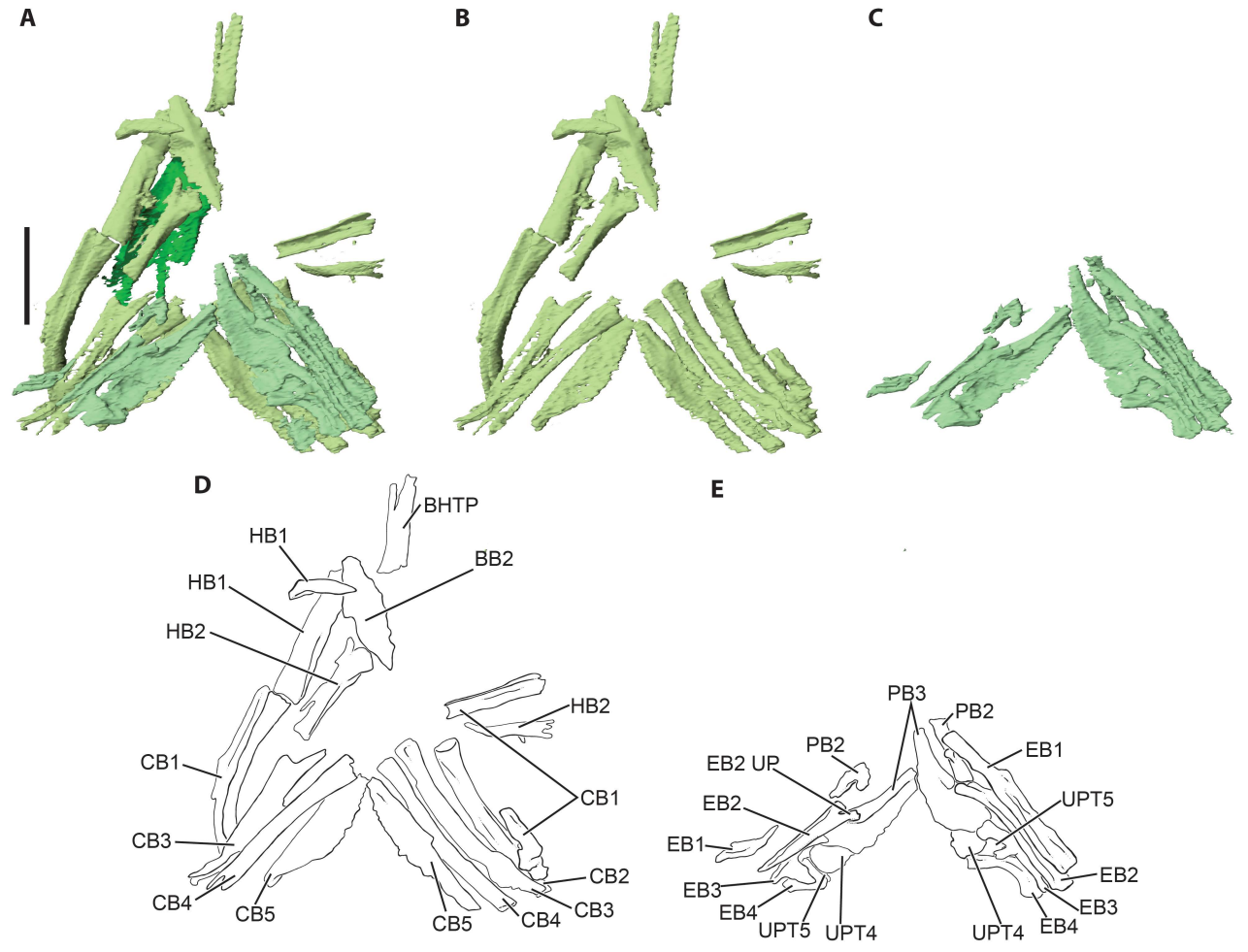
A
B
C
D
BHTP
HB1
BB2
HB1
HB2
HB2
CB1
CB1
CB3
CB2
CB4
CB5
CB5
CB4
CB3
E
PB3
PB2
PB2
EB1
EB2 UP
UPT5
EB2
EB1
EB2
EB3
EB4
EB3
UPT5
UPT4
UPT4
EB4

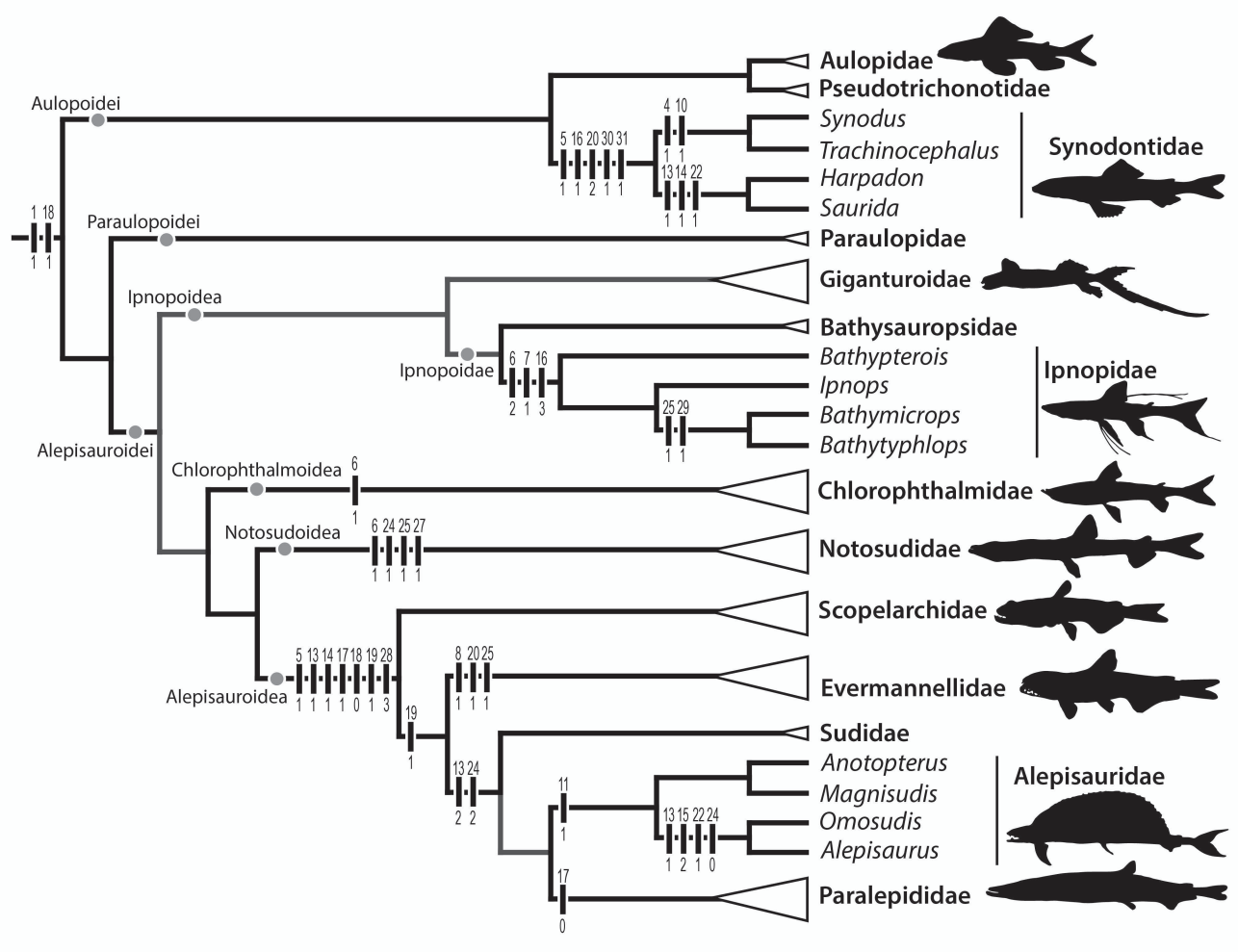
Aulopidae
Pseudotrichonotidae
Synodus
Trachinocephalus
Harpadon
Saurida
Synodontidae
Paraulopidae
Giganturoidae
Bathysauropsidae
Bathypterois
Ipnops
Bathymicrops
Bathytyphlops
Ipnopidae
Chlorophthalmidae
Notosudidae
Scopelarchidae
Evermannellidae
Sudidae
Anotopterus
Magnisudis
Omosudis
Alepisaurus
Alepisauridae
Paralepididae
Aulopoidei
Paraulopoidei
Ipnopoidea
Ipnopoidae
Alepisauroidei
Chlorophthalmoidea
Notosudoidea
Alepisauroidea
1 18
1 1
5 16 20 30 31
1 1 2 1 1
4 10
1 1
13 14 22
1 1 1
6 7 16
2 1 3
25 29
1 1
6
1
6 24 25 27
1 1 1 1
5 13 14 17 18 19 28
1 1 1 1 0 1 3
8 20 25
1 1 1
19
1
13 24
2 2
11
1
13 15 22 24
1 2 1 0
17
0

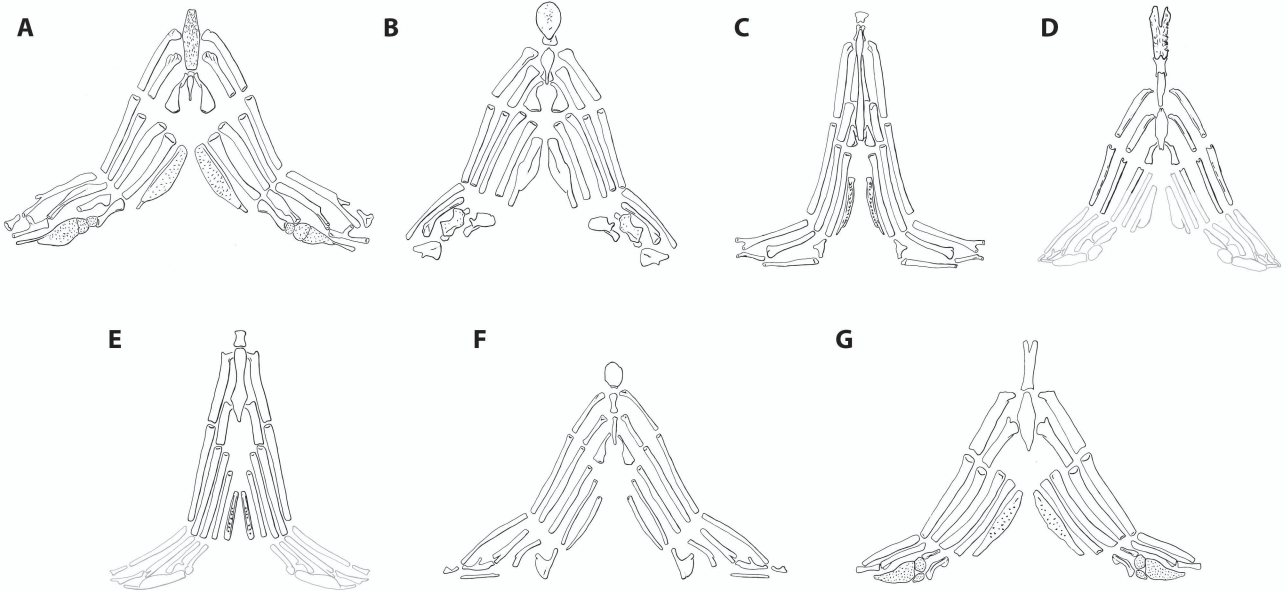
A
B
C
D
E
F
G

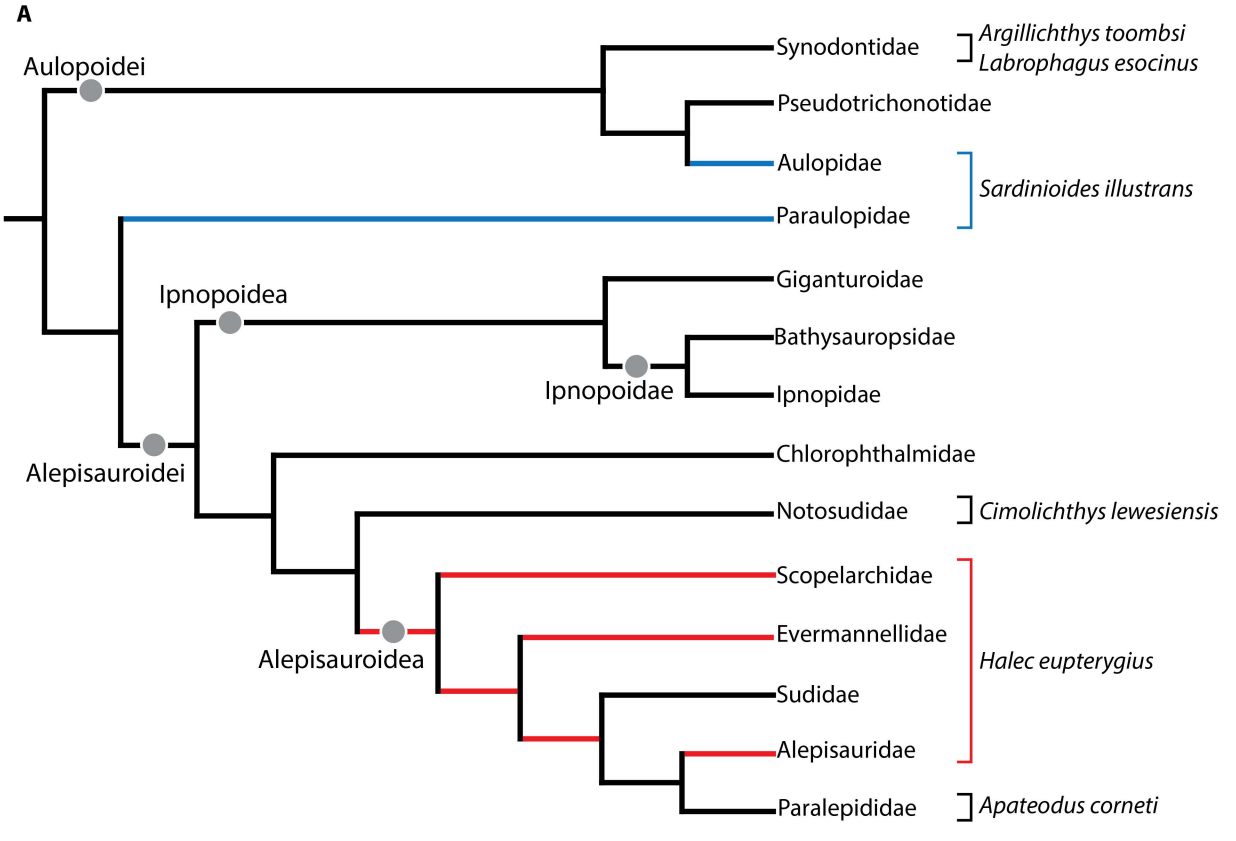
A
Aulopoidei
Synodontidae
Argillichthys toombsi
Labrophagus esocinus
Pseudotrichonotidae
Aulopidae
Sardinioides illustrans
Paraulopidae
Ipnopoidea
Giganturoidae
Bathysauropsidae
Ipnopoidae
Ipnopidae
Alepisauroidei
Chlorophthalmidae
Notosudidae
Cimolichthys lewesiensis
Scopelarchidae
Evermannellidae
Alepisauroidea
Halec eupterygius
Sudidae
Alepisauridae
Paralepididae
Apateodus corneti

Supplementary Information

Character list pertaining to the gill arches, taken from Davis (2010)

Gill Arches

1. Second epibranchial uncinate process: absent (0), present, enlarged (1), present, not enlarged, end of second pharyngobranchial displaced posterolaterally (2), present, not enlarged, end of second pharyngobranchial displaced posteriorly (3) (Baldwin & Johnson [1], 1996; Sato & Nakabo [32], 2002).

2. Cartilaginous condyle on dorsal surface of third pharyngobranchial: PB3 with cartilaginous condyle articulating with EB2 (0), PB3 without cartilaginous condyle articulating with EB2(1) (Baldwin & Johnson [2],1996).

3. Fourth pharyngobranchial toothplate: UP4 present (0), UP4 absent (1) (Baldwin & Johnson [3], 1996).

4. Articulation of first pharyngobranchial: PB1 articulates at distal tip of EB1 (0), PB1 articulates at proximal base of cartilaginous tip of EB1 (1) (Baldwin & Johnson [4], 1996).

5. Gill rakers or toothplates: Gill rakers long, lathlike (0), gill rakers present as tooth- plates (1), single elongate gill raker on EB1 (2) (Baldwin & Johnson [5], 1996).

6. Second pharyngobranchial with extra uncinate process: PB2 without extra uncinate process (0), PB2 without extra uncinate process but with expanded proximal base (1), PB2 with extra uncinate process (2) (Baldwin & Johnson [6], 1996).

7. Second pharyngobranchial toothplate: UP2 present (0), UP2 absent (1) (Baldwin & Johnson [7], 1996).

8. Second pharyngobranchial uncinate process: PB2 with short uncinate process

(0), PB2 with long uncinate process (1) (Baldwin & Johnson [8], 1996).

9. Uncinate process of second epibranchial adjacent to second epibranchial: EB2 uncinate process diverges from EB2 as it approaches PB3; PB2 oriented anteromedial to posterolateral (0), EB2 uncinate process adjacent to EB2 as both approach PB3; PB2 oriented anterior to posterior (1) (Baldwin & Johnson [9], 1996).

10. Articulation between uncinate processes of first epibranchial and second pharyngobranchial: EB1 and PB2 articulate via uncinate processes (0), uncinate process of EB1 does not articulate with that of PB2 (1), uncinate process on EB1 absent (2) (Sato & Nakabo [43], 2002).

11. Third pharyngobranchial produced: PB3 not extending anteriorly beyond the tips of EB1 and PB2 (0), PB3 extending anteriorly beyond the tips of EB1 and PB2 (1) (Baldwin & Johnson [10], 1996).

12. Bony ridge on dorsal surface of third pharyngobranchial: absent (0), present (1) (Sato & Nakabo [34], 2002).

13. Distribution of PB3 teeth: UP3 covering large area of ventral surface of PB3 (0), UP3 restricted to lateral edge of ventral surface of PB3 (1), UP3 absent (2) (Baldwin & Johnson [11], 1996).

14. Size of PB3 teeth: small (0), large (1) (Baldwin & Johnson [12], 1996).

15. First pharyngobranchial: PB1 normal or reduced (0), PB1 very long (1), PB1 absent (2) (Baldwin & Johnson [13], 1996; Sato & Nakabo [38], 2002).

16. Fourth epibranchial morphology: EB4 has a slender proximal end and an uncinate process attached to the fourth levator externus (0), end of EB4 slender, but lacks an uncinate process (1), EB4 has an expanded proximal end capped with a large band of cartilage and an uncinate process at the middle (2), proximally expanded EB4 lacking an uncinate process (3) (Sato & Nakabo [44], 2002).

17. Ossification of first epibranchial and ceratobranchial: well ossified and capped by a proximally short cartilage (0), ossification weak, proximal cartilaginous portions long (1) (Sato & Nakabo [46], 2002).

18. Fifth epibranchial: EB5 absent (0), EB5 present (1) (Baldwin & Johnson [14], 1996; Sato & Nakabo [45], 2002)

19. Dentition of fifth ceratobranchial: teeth scattered all over anterodorsal surface (0), teeth restricted to medial edge of anterodorsal surface (1), teeth restricted to medial edge of anterodorsal surface (2), without teeth (3) (Baldwin & Johnson [15], 1996).

20. Shape of fifth ceratobranchial: ceratobranchial 5 not V-shaped (0), ceratobranchial 5 V-shaped, the medial limb slender (1), ceratobranchial 5 V-shaped, the medial limb robust (2) (Baldwin & Johnson [16], 1996).

21. Gap between the fourth basibranchial cartilage and fifth ceratobranchials: no gap (0), gap between ceratobranchial 5s and BB4 cartilage, ceratobranchial 5s not articulating with reduced BB4 (1), ceratobranchial 5s separated from main body of BB4 by tail or small nubbins of cartilage extending posteriorly from BB4 (2) (Baldwin & Johnson [17], 1996).

22. Third basibranchial extends beyond fourth basibranchial cartilage: BB3 terminates beneath the anterior end of BB4 cartilage(0), BB3 terminates beyond the posterior end of BB4 cartilage(1) (Baldwin & Johnson [18],1996).

23. Fourth basibranchial ossified: cartilaginous (0), ossified (1) (Baldwin & Johnson [19], 1996).

24. Elongate first basibranchial: BB1 not elongate (0), BB1 elongate, ossified (1), BB1 usually elongate, comprising a short ossified anterior segment followed by a long posterior cartilage (2) (Baldwin & Johnson [20], 1996).

25. Elongate second basibranchial: not elongate (0), elongate (1) (Baldwin & Johnson [21], 1996).

26. Gillrakers or toothplates on third hypobranchials: present on HB3 (0), absent on HB3 (1) (Baldwin & Johnson [22], 1996).

27. Gillrakers or toothplates on basibranchials: lacking on basibranchials (0), present on BB2, sometimes BB1 and BB3 (1) (Baldwin & Johnson [23], 1996).

28. Gill rakers on medial surface of gill arches: present (0), absent on first arch only (1), present on first hypobranchial only (2), absent (3) (Sato & Nakabo [50], 2002).

29. Ligament between first hypobranchial and ventral hypohyal: not ossified (0), ossified (1) (Baldwin & Johnson [24], 1996).

30. First hypobranchial with ventrally directed processes: without ventrally directed processes (0), with a ventrally directed process (1) (Baldwin & Johnson [25], 1996).

31. Second hypobranchial with ventrally directed process: without ventrally directed processes (0), with a ventrally directed process (1) (Baldwin & Johnson [26], 1996).

32. Third hypobranchials fused ventrally: not fused (0), fused (1) (Baldwin & Johnson [27], 1996).

Specimen Name	Specimen Number	Filter Material	Filter Thickness	Current	kV	Resolution (mm)
†***Apateodus corneti***	RGM 446950	Copper	2.5	200	196	0.1070
†***Argillichthys toombsi***	NHMUK PV OR P42519	Copper	2.5	184	199	0.0430
†***Aulopopsis depressifrons***	NHMUK PV OR P26712	Copper	2.5	161	215	0.0320
†***Cimolichthys lewesiensis***	NHMUK PV OR P5491	Copper	2.5	158	209	0.0567
†***Halec eupterygius***	NHMUK PV OR P5662	Copper	2.5	164	210	0.0561
†***Labrophagus esocinus***	CAMSM TN 4286	Tin	1.25	170	205	0.0863
†***Sardinioides illustrans***	NHMUK PV OR P3977	Copper	2.5	192	200	0.0503

Table 1: Parameters used for scanning specimens. 3142 projections were acquired for each specimen.

Specimen Name	
†*Apateodus corneti*	3?1?101010 00??0{0/3}0?20 ??001?1??0 00
†*Argillichthys toombsi*	1?00110100 0100030?00 ??000?1??1 10
†*Aulopopsis depressifrons*	1???10?0?? ????0?0??? ??000?1??0 00
†*Cimolichthys lewesiensis*	?????????? ?????????? ???11?1??? ?0
†*Halec eupterygius*	????1????? ????????20 ??000?1??? ?0
†*Labrophagus esocinus*	1????0000? ????0?0?00 ??000?1??1 10
†*Sardinioides illustrans*	1?0??0?000 0100?00?00 ??000????? ??

Table 2: Character codings for fossil taxa included in this analysis. For corresponding character list, see Supplementary Information.